

Monte-Carlo Event Generators at NLO

John Collins*

*Physics Department, Penn State University,
104 Davey Laboratory, University Park PA 16802, U.S.A.*

(Dated: 8 October 2001)

A method to construct Monte-Carlo event generators at arbitrarily non-leading order is explained for the case of a non-gauge theory. A precise and correct treatment of parton kinematics is provided. Modifications of the conventional formalism are required: parton showering is not exactly the same as DGLAP evolution, and the external line prescription for the hard scattering differs from the LSZ prescription. The prospects for extending the results to QCD are discussed.

PACS numbers: PACS 12.38.Bx, 13.87.-a

I. INTRODUCTION

There are two contrasting approaches to making perturbative predictions from QCD. The first consists of the analytic (or matrix element) methods [1], where a factorization theorem is used to write inclusive cross sections in terms of perturbatively calculable hard-scattering coefficients and of parton densities and fragmentation functions. The second approach is that of the Monte-Carlo event generator [2]. Now, the analytic methods have the advantage of permitting calculations to arbitrary non-leading order, and thus of allowing a systematic improvement in the accuracy of calculations. In contrast, the Monte-Carlo methods have the advantage of generating complete events and of implementing QCD predictions for the detailed structure of the final state, but at the expense of model dependence in the hadronization. But up to now, a systematic method of incorporating higher order corrections, in powers of α_s , has not been available for the Monte-Carlo method. Currently available event generators incorporate hard scattering and evolution at the leading order (leading-logarithm approximation, and somewhat beyond), and, although some implementations of non-leading corrections have been made [3, 4], there has not so far been devised a general method.

It is of course highly desirable to extend the algorithms in the event generators to non-leading order. Once this aim has been achieved, one can use the highest precision QCD calculations while retaining the advantages of the event generators. The many currently available NLO and NNLO analytic calculations of Feynman graphs will of course continue to be used; they will merely need to be reformulated to be used in event generators.

In Ref. [5], I proposed a subtractive approach and applied it to the simple, but phenomenologically important, process of photon-gluon-fusion in deep inelastic scattering. This approach was intended to be generalized to provide a complete solution to the problem of non-leading corrections to event generators. Unfortunately, a full treatment of QCD is quite hard, because of the need to treat soft gluon effects. So the present paper restricts its

*Electronic address: collins@phys.psu.edu

attention to providing a complete treatment within a model theory where only collinear configurations are important.

For ease of exposition, only the rather unphysical case of ϕ^3 theory in 6 space-time dimensions will be discussed, but the methods immediately generalize to any non-gauge theory¹. In such a theory, we will see in complete generality how to construct Monte-Carlo event generators for e^+e^- annihilation with the inclusion of arbitrarily non-leading order corrections, in the hard scattering and in the final-state showering. The irreducible errors are then due to power-law corrections to the hard scattering and evolution kernels. The extension to initial-state showering should be relatively elementary.

The general principle of the method is to generate extra kinds of hard interaction and splitting kernels corresponding to non-leading-order corrections, and to apply subtractions to allow for the effect of lower-order terms coupled to showering. The subtractions are applied point-by-point in momentum space with proper allowance for correct parton kinematics, so that the NLO corrections form completely well-behaved functions. This is in contrast to the subtractive methods used in parton-level Monte-Carlo calculations for infra-red-safe observables, as in Ref. [7]. In those methods the NLO corrections are singular distributions which can only be used to calculate suitably infra-red-safe observables. The new method is applicable to general cross sections.

The viewpoint in this paper can be characterized as “static”: It asks what the value is of a certain sum of integrals for the cross section. This contrasts with the more dynamic viewpoint normally used in discussions of event generators, where the primary concept is the evolution of partonic states. An actual implementation of the methods of this paper will recover this dynamic point-of-view, for that is inherent in the structure of the Monte-Carlo algorithms derived from the static Feynman graph structure.

Although the model theory treated in this paper is relatively simple, even this case already poses some quite non-trivial difficulties if one is to solve completely and reliably the problem of obtaining corrections for use in an event generator. Arbitrarily high-order Feynman graphs are being approximated in such a way that an estimate of the cross section for producing N particles needs computational resources proportional to N , even though a brute force calculation requires resources more like $N!$.

Since the mathematical structure worked out in this paper is quite general, I hope that the same structure and proof will apply in many situations, with minor modifications. The essential problem to be solved in this and any other problem in asymptotic behavior in quantum field theories (including QCD) is to find an economical way of treating the large multiplicity of different regions that give the leading contributions from a single graph. Any economical method must treat exactly one region at a time, and involve only simple and very general relations to other regions.

In addition, the methods used in the proof should be of use in algorithms for QCD calculations (both numeric and symbolic). Because of the many singularities in unintegrated graphs, it is important to have robust control over the sizes of the contributions from the different regions, and to have a very concrete definition of subtracted integrands, which are to be well-behaved numerically. The methods of proof in this paper, with their simple but strongly recursive structure, are appropriate for generalization for this purpose.

In Sec. II are summarized some of the general ideas used in this paper. Then, in Sec. III,

¹ In a theory with fermionic fields, for example, spin effects can be included by the method I proposed in [6].

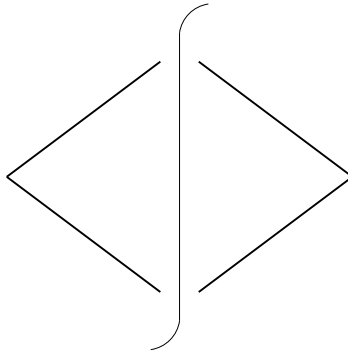


FIG. 1: e^+e^- annihilation to 2 partons in lowest order.

we define the cross section that is to be treated and construct the basic elements that are used in the algorithm. The basic ingredient used to construct the factors in the factorization theorem is an approximation where the external lines of the hard-scattering are set on-shell. Precise definitions of this approximation are given in Sec. IV. The definitions are arranged to be suitable for a Monte-Carlo event generator, where it is essential that parton 4-momentum is exactly conserved; approximations that change the total 4-momentum of the scattering have to be used carefully. Before giving the general proofs, we show, in Sec. V, how the methods are applied to specific Feynman graphs. In Sec. VI, a general proof of factorization is given in the form that it is needed to obtain an algorithm for a Monte-Carlo event generator. This section also includes a proof of the collinear safety of the hard scattering and the integrated jet factors, as well as a discussion of the renormalization group properties of the factors in the factorization theorem. These are all essential to an actual implementation of the algorithm. In Sec. VII, we then obtain the Monte-Carlo algorithm; this is the culmination of the theoretical treatment. Sec. VIII shows examples of complete calculations of corrections to the hard-scattering, at NLO. Finally, some conclusions are presented in Sec. IX and some of the difficulties that remain in extending the method to QCD are explained.

II. MAIN FEATURES OF THE NEW METHOD

A. Previous methods

The methods used to treat higher-order corrections in the analytic methods, even within a Monte-Carlo approach [7], do not directly translate to methods for event generators. One of the reasons is the way in which approximations are made on the kinematics of events. Consider, for example, the production of two or three partons (in e^+e^- -annihilation). The lowest order graph for 2-parton production, shown in Fig. 1, is assigned to an exactly back-to-back configuration. In the lowest order graph for 3-parton production, Fig. 2, the 3 partons are not back-to-back. However there is a singularity in the 3-parton calculation when pairs of the final-state particles approach each other and make a 2-jet configuration. This part of the cross-section is really a 2-jet process with an order α_s contribution to the fragmentation of one of the jets.

In the standard calculation of the hard-scattering coefficient for 3-parton configurations, a subtraction is made of a fragmentation factor times the 2-parton cross section, which is

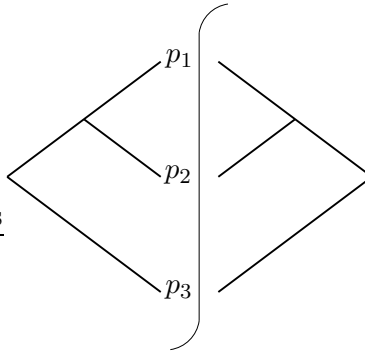


FIG. 2: A graph for e^+e^- annihilation to 3 partons.

localized in exactly the back-to-back situation. Let \mathbf{q}_T be a transverse momentum that parameterizes the deviation from a back-to-back configuration. Then the resulting contribution to the hard-scattering coefficient for the 3-jet cross section is of the form:

$$\left(\frac{a \ln q_T^2 + b}{q_T^2} \right)_+ + c \delta^{(2)}(\mathbf{q}_T), \quad (2.1)$$

plus some irrelevant non-singular terms. Without the $+$ prescription, the cross section has a divergent integral over \mathbf{q}_T . Although the subtraction at $q_T = 0$ produces a valid, integrable distribution (or generalized function), it does not produce an ordinary function. To implement a 3-jet cross section in an event generator one should have an ordinary function, not a distribution.

A related difficulty is that after showering and hadronization of the final-state partons, the two graphs, Figs. 1 and 2, produce hadrons in overlapping regions: one cannot distinguish between an event that is derived from exactly back-to-back partons, as in Fig. 1, and an event derived from an almost back-to-back configuration from Fig. 2. However, the distribution in Eq. (2.1) does make such a distinction. Moreover from the large q_T tail of the hadronization of the 2-jet cross section one obtains final states with 3 (or more jets).

The simplest solution to these problems is to compute an infra-red safe observable, like thrust. This is commonly done with jet production in e^+e^- annihilation [7]. But this is not suitable in an event generator, where exclusive final states are generated and arbitrary observables can be estimated.

Another method is commonly used in hadron-hadron collisions, where the cross sections for all jet observables involve parton densities, so that purely perturbative calculations are never IR safe. This method is to convolute Eq. (2.1) with some kind of smearing function, that intuitively is supposed to represent intrinsic transverse momentum of partons relative to corresponding hadrons. Without further justification, this is just an ad hoc prescription that is used in an attempt to model a physical phenomenon that is clearly present. Furthermore, some of the q_T smearing is contained in higher-order corrections to the hard scattering. To implement a valid calculation, it is necessary to devise a subtraction method that is derived from the underlying field theory and that prevents double counting; in a sense this gives a correct method to implement q_T smearing.

One very different approach that has been used [3] to implement NLO corrections in event generators is to reweight events after they have been generated, so that the hard scattering cross section is renormalized to the value known from analytic calculations. In addition,

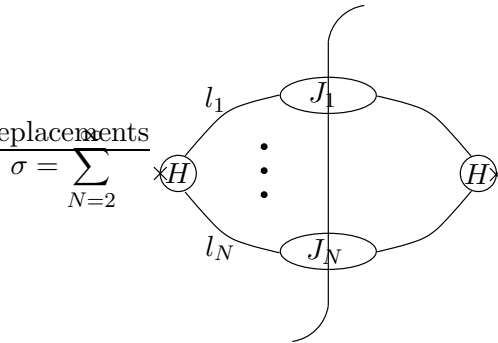


FIG. 3: General leading-power contribution to cross section

the unsubtracted NLO correction is used to populate regions of phase space not filled by showering the partons associated with the LO cross section. This method does not readily generalize.

B. Overall structure of new method

The basic idea of the new method is that the subtractions should be computed with the correct parton kinematics, rather than a zero-transverse-momentum approximation such as is implicit in the +-distribution in Eq. (2.1). This means that we must always remember that graphs like Figs. 1 and 2 do not fully represent the physics. The parton lines going into the final state should really be replaced by bubbles representing hadronization, as in Fig. 3, which represents the most general leading region.

Apart from such implementation issues, the basis of the method is the usual factorization theorem: As illustrated in Fig. 3, the leading power contributions involve a hard scattering convoluted with jets, each jet being induced by a single parton of relatively low virtuality. The algorithm for the event generator makes recursive use of the factorization theorem by applying it to each of the jets whenever the invariant mass of the parton initiating the jet is much larger than a typical hadronic mass. In this second application of factorization to the jets, the hard-scattering coefficients are equivalent to the DGLAP splitting kernels.

Current event generators are based on a leading-order approximation which involves the use of the lowest order expansion of the hard-scattering and splitting kernels together with Sudakov form factors that encode the renormalization-group transformation between the potentially widely different scale in the different applications of factorization.

What has been gained by the use of factorization is the ability to compute an arbitrarily large number of high-order Feynman graphs in a time that is merely proportional to the number of particles in the final state. The price of this is that approximations have been made, both as regards the kinematics of individual graphs and as regards the subset of graphs that is calculated. It is the proof of the factorization theorem that shows that the approximations are valid and useful.

At each stage of the algorithm, there are errors due to higher-order corrections to the relevant hard scattering. The higher-order contributions to the cross section are computed by subtracting from the bare graphs contributing to the H subgraphs in Fig. 3 the contributions at the same order that are allowed for in the lower-order calculation combined

with showering. To devise an algorithm one must: (a) define precisely what is being computed, (b) define precisely the kinematic approximations used in the hard scattering, and (c) implement the subtractions point-by-point in momentum space. The subtraction terms are computed with the same kinematics as the bare term, to satisfy the last requirement, while the kinematic approximations are only used in the computation of the numerical values of the matrix elements, but not in defining the parton momenta. A similar treatment of initial-state showering will require us to employ parton densities differential in transverse momentum, or some equivalent concept.

Once the method is formulated properly for the higher order corrections to the hard scattering, it is readily extended to the evolution kernels, as we will see.

One potential problem is that, as is well known, subtraction methods tend to generate terms in the cross section that are negative. The reason is that if, as is possible, a next-to-leading (NLO) correction decreases the cross section compared with the leading-order (LO) cross section, then the NLO term is negative. The virtual corrections to the hard scattering can simply be added to the LO term; in the method proposed in this paper, these virtual corrections will always be collinear and infra-red safe, even in QCD — see the work of Collins and Hautmann [8, 9] — since the collinear and soft pieces are supposed to be subtracted. Thus the virtual corrections cause no problems of positivity.

As for the real NLO corrections, they are treated as generating a separate class of events. Where their contribution to the differential cross section is negative, these events must be generated with negative weight. This is often considered undesirable, but as explained in [5], this is actually acceptable for most purposes, provided that only a reasonably small number of events with moderate negative weights is generated. Then the negative-weight events are outweighed by larger positive contributions to a binned cross section. What is not acceptable is to have the cross section be obtained as a cancellation of relatively much larger positive and negative contributions. An extreme example of this is given by Eq. (2.1). There the distribution $(1/q_T^2)_+$ consists of an unsubtracted $1/q_T^2$ term, which integrates to positive infinity, and a delta function with an infinite negative coefficient. It is also essential that all regions of final-state momentum space that are populated by negative-weight NLO events are also populated by positive-weight LO events; thus the cancellations that give a positive physical cross section occur point-by-point rather than between neighboring bins. Both these conditions are fulfilled by my algorithm.

In addition, the Monte-Carlo formalism contains some cut-off functions. When the higher-order corrections are included, there is a renormalization-group invariance under changes of the cut-off functions, and these can be adjusted [5] to at least reduce the number of negative-weight events.

III. DEFINITION OF PROBLEM

A. Model for e^+e^- annihilation

Let us use ϕ^3 theory in 6 space-time dimensions, which has the Lagrangian

$$\mathcal{L} = \frac{1}{2}\partial\phi^2 - \frac{m^2}{2}\phi^2 - \frac{g}{6}\phi^3. \quad (3.1)$$

In addition, to mimic an interaction with a photon, let us suppose that there is a weakly interacting scalar field A , which will be called a photon, and that the interaction with the

ϕ field is proportional to Aj where the “current” j is the renormalized operator² $[\frac{1}{2}\phi^2]$. To emphasize the analogy that is intended with QCD, let us call ϕ the “parton” field.

The process we work with is an analog of e^+e^- annihilation to hadrons. It will be necessary to consider various cross sections (including, for example, the total cross section, jet cross sections and completely exclusive cross sections), so to unify the treatment I define a weighted cross section by

$$\sigma[W] = K \sum_f W(f) \int d^6x e^{iq \cdot x} \langle 0 | j(x) | f \rangle \langle f | j(0) | 0 \rangle. \quad (3.2)$$

Here q^μ is the total incoming momentum, $j(x)$ is the current operator defined above, and K is a standard factor that depends only on the leptonic variables. The sum over f denotes an integral and sum over all final states³, and $W(f)$ is a weighting function that defines the particular cross section under consideration. All cross sections can be obtained if $\sigma[W]$ is known for all W . Let us work in the overall center-of-mass frame, $q^\mu = (Q, \mathbf{0})$.

Examples of the choice of the weighting function are:

- The total cross section, given by $W = 1$ for all final states.
- The 2-jet cross section, for which $W(f) = 1$ for all final states containing exactly two jets (given some definition of a jet), and $W(f) = 0$ otherwise.
- A fully differential two particle cross section, for which $W(f)$ is the appropriate δ function for two particle final states, and for which $W(f) = 0$ for final states containing three or more particles.

B. Leading-power contributions

Our aim is to decompose the cross section into its completely exclusive components, and to obtain an algorithm for calculating them to the leading power in Q . Now, the usual power-counting theorems of Libby and Sterman [10], which are formulated in the overall center-of-mass frame, show that the leading-power contributions to the cross section in our model theory all come from regions of the form symbolized in Fig. 3. Some lines, forming the hard subgraph H and its complex conjugate, are off shell by order Q^2 . The other lines form groups, or jets, of lines of approximately parallel momentum. These groups are labeled $J_1 \dots J_N$, and to satisfy momentum conservation there must be at least two jets, $N \geq 2$.

Unlike the case of QCD (or any other gauge theory), there are no soft subgraphs in our model ϕ^3 theory, at the leading power. This fact alone considerably simplifies the analysis in our model compared with QCD.

Individual Feynman graphs for the cross section can contribute in several different regions. For example, consider the cut graph, Γ , of Fig. 4, which has four particles in the final state, of momenta p_1, p_2, p_3 and p_4 . The graph has the following regions for leading twist contributions:

² The square bracket notation used in this context denotes a renormalized operator.

³ It is probably most useful to treat the sum and integral over final states as being over all states without regard to the constraints imposed by indistinguishability. Then the overcounting of physically identical states is to be compensated by inserting a suitable factor, which for our model theory is $1/N_f!$, where N_f is the number of final-state particles.

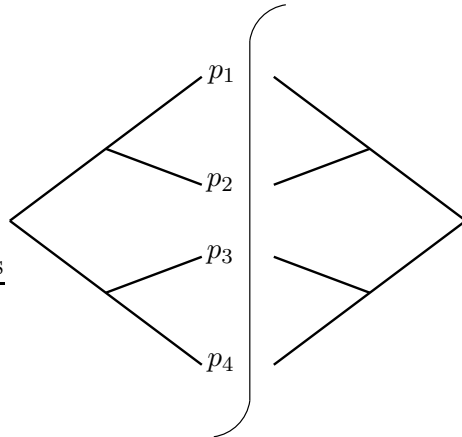


FIG. 4: Graph with several leading regions

1. p_1 and p_2 are almost parallel, and p_3 and p_4 are also almost parallel.
2. p_3 and p_4 are almost parallel, but p_1 and p_2 are at wide angle.
3. p_1 and p_2 are almost parallel, but p_3 and p_4 are at wide angle.
4. All the final-state momenta are at wide angles with respect to each other.

There are of course contributions from intermediate regions, and these give the leading-logarithmic part of the cross section. The techniques of our proof will avoid any need to consider these intermediate regions explicitly.

C. Summary of proof of factorization and application to event generator

A summary of the proof of the factorization theorem in perturbation theory is as follows:

1. Write the cross section as a sum over graphs Γ .
2. Write each graph as a sum of terms $C_R(\Gamma)$, one for each of its leading regions R :

$$\Gamma = \sum_{\text{regions } R} C_R(\Gamma) + \text{non-leading power of } Q. \quad (3.3)$$

3. Sum over all possibilities:

$$\begin{aligned} \sigma[W] &= K \sum_{\text{final states } f} \sum_{\text{graphs } \Gamma} \Gamma W(f) \\ &= K \sum_f \sum_{\Gamma, R} C_R(\Gamma) W(f) + \text{non-leading power of } Q. \end{aligned} \quad (3.4)$$

Here K is the same overall factor that we used in Eq. (3.2).

4. Now $C_R(\Gamma)$ (to be defined later) is the product of a hard part and a set of jet factors, with these factors corresponding to particular contributions to the subgraphs H and J_i in Fig. 3. The sum over graphs and regions can be reformulated as independent

sums over the hard part and the jet subgraphs, and this gives the desired factorization theorem:

$$\sigma[W] = K \sum_f \sum_N \hat{H}_N \times \Delta \times \prod_{j=1}^N J_j W(f) + \text{non-leading power.} \quad (3.5)$$

Here, the hard part is denoted by \hat{H}_N , with a hat over the H . The hat indicates that the contributions to the hard part are not obtained simply as the contributions of appropriate Feynman graphs in a certain region of momentum space. Instead, as we will see, they are obtained from the relevant Feynman graphs with the aid of a subtraction procedure that prevents double counting. The factor Δ is a Jacobian, whose calculation we will see later; it relates the integration over the massless final-state momenta of \hat{H}_N to the integration over the correct and off-shell parton momenta.

5. It is convenient to adjust the normalizations to give a formula that has a convenient interpretation as a hard-scattering factor times jet factors that are normalized to be probabilities—see Eq. (6.45) below.

In a Monte-Carlo event generator, all integrals over final states are done by a Monte-Carlo technique. After generating the distribution of partons associated with the hard scattering, the distribution over invariant mass for each jet-initiating parton l_j is computed. Because of the collinear safety of total cross sections, this is a perturbative calculation when the virtuality of l_j is large. Then a further application of the factorization theorem is made to each jet, whenever the invariant mass of the initiating parton of the jet is large enough for the use of perturbative methods. This procedure is applied recursively until all the generated partons have low invariant mass. After that a hadronization model is applied, so that a hadronic final state is generated. Finally, the weight function $W(f)$ may be applied, to define a particular cross section. Since the weight function is only applied at the last stage, all the previous steps can be implemented independently of the cross section being computed. Hence the events can in fact be generated without regard to the weight function; the weight function simply provides a convenient tool to unify all cross section calculations into a single formula.

D. Comments

The proof is given only in perturbation theory, but with a treatment of all orders at the leading power. Nevertheless the structure that is derived is evidently more general. Thus one can conjecture that a better and less perturbative treatment is possible. In particular, it is very natural that the structure of Fig. 3 should hold beyond perturbation theory.

Factorization is needed so that the structure of the algorithm for generating events is simple. One important feature is that the hard scattering contribution from each region is computed in the approximation that its external lines have zero virtuality. Thus the computation of the hard-scattering can be done independently of the subsequent computation of the properties of the jets. This approximation is good up to the claimed power-law correction when the virtualities of the jet-initiating partons are low. When the virtualities of these partons get large, the approximation worsens. But then, as we will see, the higher-order corrections to the hard scattering correctly handle this situation, and compensate the errors.

For the decomposition of the graphs into a sum over regions, phase-space slicing is the most obvious method. However it does not produce the desired result, since the errors are fairly hard to control, and the errors tend to be quite non-optimal⁴. This will lead us to use a more formal subtraction method.

Essential requirements on its implementation appear to be:

- Each particular subgraph for H and J_j gives the same result in all contexts, independently of the graph Γ from which the subgraph arises. This allows the manipulations between Eqs. (3.4) and (3.5) to work.
- The space of final states factorizes into parts associated with the partonic final states of the hard scattering and parts associated with the final states of each jet. Then factorization for the cross section follows from factorization for the amplitudes in each region. Again this is needed so that the manipulations between Eqs. (3.4) and (3.5) work.
- The quantity $C_R(\Gamma)$ that defines the contribution of a graph Γ in a region R must be an ordinary function, not a singular distribution. Then the integral over final states can be implemented by a Monte-Carlo method.

E. Errors

It is a little complicated to explain what are the errors on the approximations we make. This is an important issue to get correct, because if an event generator is used to make predictions that are compared with experiment, we need to understand the significance of deviations between the data and the predictions.

First observe that the amplitudes are treated with the correct final states but with an approximation on the values of the amplitudes. The power counting theorems of Libby and Sterman show that the total cross-section is computed up to an error that is suppressed by a power of Q . Moreover this cross section is correctly decomposed into its exclusive components. So the obvious expectation is that the differential Monte-Carlo cross section differs from the exact cross section by a power suppressed error:

$$\sigma_{\text{exact}}[W] - \sigma_{\text{calculated}}[W] = \sigma_{\text{exact}}[W] \times O(m/Q)^p \text{ (incorrect estimate)}. \quad (3.6)$$

Here m is a typical hadronic mass scale, and p is some positive number. For most final states, this estimate is indeed correct, since the approximations used are good to power-law accuracy in each leading region.

However, there are other, non-leading regions, and for the theories under consideration this means regions that are not of the form of Fig. 3. The approximations we made are not valid in these regions, so a substantial deviation between theory and experiment can occur in a non-leading region. On the other hand, a non-leading region gives a power-suppressed contribution to the cross section; that is exactly what it means to say that the region is non-leading. So typically we will have small contributions to the cross section from such a region.

⁴ The word “error” in this context means the difference between the exact value of a graph and the approximation used in the sum over regions.

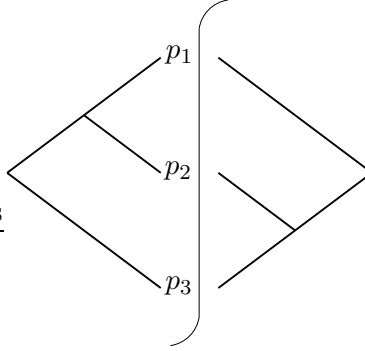


FIG. 5: A graph for e^+e^- annihilation to 3 partons with no singular leading regions.

Therefore we need to modify the error estimate. The following is one possibility:

$$\sigma_{\text{exact}}[W] - \sigma_{\text{calculated}}[W] = \sigma_{\text{total}} \times O(m/Q)^p \text{ (weak estimate)}. \quad (3.7)$$

This says that the error is power suppressed with respect to the total cross section. Unlike the previous estimate, it is excessively weak, since the non-leading regions will populate only certain regions of the space of final states. The simplest correct estimate is

$$\sigma_{\text{exact}}[W] - \sigma_{\text{calculated}}[W] = \sigma_{\text{calculated}}[W] \times O(m/Q)^p + \text{terms for non-leading regions}. \quad (3.8)$$

This says that the errors come from two sources: power-suppressed errors in the approximations, and contributions from non-leading regions. It leaves open the issue of exactly which hadronic final states are populated by the non-leading partonic regions.

An example of the issues can be seen with the aid of the graph of Fig. 5. The only leading region for this graph is the wide angle region, where the partonic final state makes 3 jets. It also has non-leading regions. Among these are 2-jet regions, where 2 partons are close in angle. Only one propagator has a small denominator, so the graph's contribution is much smaller than the contribution of graphs like those of Fig. 2, where two denominators are small. Since there are other contributions to the cross section that are bigger, we see that the graph makes a power-suppressed contribution to the 2-jet region. In addition, there is a region where parton p_2 is soft, i.e., has all its momentum components much less than Q . This region would be leading in QCD, if the soft parton were a gluon, but the region is non-leading in a non-gauge theory. However, the kinematic region it gives in the final state is not necessarily populated by the leading regions, so this case gives a non-trivial example of the last term on the right-hand side of Eq. (3.8).

IV. KINEMATICS OF HARD SCATTERING

The core of the proof of factorization is a treatment of the sum over leading regions for an individual graph in Eq. (3.3). Each term $C_R(\Gamma)$ is defined by an appropriate kinematic approximation and a subtraction procedure. Given this definition, one must prove the error estimate in Eq. (3.3). Various properties of the kinematic approximations and the subtractions are needed to obtain the Monte-Carlo algorithm and the methods for the calculation of non-leading corrections. These properties ensure that the combinatorial part of the proof, between Eqs. (3.4) and (3.5), actually works.

In this section we define the approximation associated with a particular region, and derive its important properties.

A. Approximation

Consider a generic leading-power contribution from a particular graph for the cross section, as symbolized in Fig. 3. From it we will now construct an approximation that is suitable for obtaining a factorization theorem and a Monte-Carlo implementation. The main idea of the approximation is to replace the external momenta of the hard subgraph H by on-shell massless momenta, and also to set the masses of the internal propagators of H to zero. Since the approximation will be integrated to a region outside of its domain of validity, it will be necessary to give precise definitions of the transformation from the exact momenta to the massless approximated momenta and to compute the Jacobian of the transformation.

Let $\Gamma[W]$ denote the particular graph that is being computed, and let it be decomposed into subgraphs corresponding to a particular region R of the form of Fig. 3, with H_R being the hard subgraph and with $J_{R1} \dots J_{NR}$ being the jet subgraphs:⁵

$$\Gamma[W] = \int dL(p; q, m) H_R(l) \prod_j J_{Rj}(p_j) W(f). \quad (4.1)$$

Here the momenta are defined as follows:

- The final-state particles of jet subgraph J_{Rj} are $p_{j,1}^\mu, \dots, p_{j,n_j}^\mu$, where n_j is the number of final state lines of J_{Rj} .
- Then p_j , with one subscript, denotes the collection of these n_j momenta, i.e., $p_j^\mu = (p_{j,1}^\mu, \dots, p_{j,n_j}^\mu)$. The sum of these momenta is $l_j = \sum_{i=1}^{n_j} p_{j,i}$, which is the momentum of the line joining J_{Rj} to the hard subgraph H_R .
- The symbol p , with no subscripts denotes the collection of all momenta of the final state particles.
- The symbol l , with no subscript, denotes the collection of the l_j 's, i.e., $l^\mu = (l_1^\mu, \dots, l_{NR}^\mu)$. The sum of these momenta is the photon momentum: $\sum_{i,j} p_{j,i}^\mu = \sum_j l_j^\mu = q^\mu$.

The symbol $dL(p; q, m)$ denotes the measure for integration over the Lorentz-invariant phase space:

$$dL(p; q, m) = \prod_{i,j} \frac{d^5 \mathbf{p}_{j,i}}{(2\pi)^5 2E_{j,i}} (2\pi)^6 \delta^{(6)}(\sum_{i,j} p_{j,i} - q), \quad (4.2)$$

with the argument m of dL denoting the mass of each of the final-state particles.

⁵ Note that the symbols H_R and J_{Rj} are not to be identified with the corresponding symbols in Eq. (3.5), although they have related meanings. In that equation, \hat{H}_N and J_j mean the fully subtracted contributions to the the hard part and the jet factors, with sums over all contributing graphs. In contrast, H_R and J_{Rj} in the current section mean the values of subgraphs of a particular graph Γ , with the subgraphs being the hard and jet subgraphs associated with a particular region R .

In Eq. (4.1), $H_R(l)$ denotes the hard factor, i.e., the expression for the product of the two subgraphs labeled H in Fig. 3 on each side of the final-state cut. The hard subgraph is to be amputated, i.e., it is without any factors for its external lines, and it is to be integrated over all its internal loop momenta.

Similarly each $J_{Rj}(p_j)$ denotes the corresponding jet factor in Fig. 3. All its external line factors are to be included. It is also to be integrated over all its internal loop momenta.

It is important to the derivation of a factorization theorem that the integration over final-state phase space in Eq. (4.1) can itself be factorized:

$$\begin{aligned}
dL(p; q, m) &= \left(\prod_j \int \frac{d^6 l_j}{(2\pi)^6} \right) (2\pi)^6 \delta^{(6)}(\sum_j l_j - q) \prod_j \left[\prod_i \frac{d^5 \mathbf{p}_{j,i}}{(2\pi)^5 2E_{j,i}} (2\pi)^6 \delta^{(6)}(\sum_i p_{j,i} - l_j) \right] \\
&= \left(\prod_j \int \frac{d^6 l_j}{(2\pi)^6} \right) (2\pi)^6 \delta^{(6)}(\sum_j l_j - q) \left(\prod_j dL(p_j; l_j, m) \right) \\
&= \left(\prod_j \int \frac{dM_j^2}{2\pi} \right) \left(\prod_j \int \frac{d^5 \mathbf{l}_j}{(2\pi)^5 2\sqrt{\mathbf{l}_j^2 + M_j^2}} \right) (2\pi)^6 \delta^{(6)}(\sum_j l_j - q) \left(\prod_j dL(p_j; l_j, m) \right) \\
&= \left(\prod_j \int \frac{dM_j^2}{2\pi} \right) \int dL(l; q, M) \left(\prod_j dL(p_j; l_j, m) \right). \tag{4.3}
\end{aligned}$$

In the first and second lines the phase space is decomposed into separate phase-space integrals $dL(p_j; l_j)$ for the final-state momenta of each jet. Then in the third and fourth lines, the integration over the l_j 's is decomposed according to the invariant mass of these momenta, so that the integration is presented as an integral over the momentum of a set of N_R particles with masses M_1, \dots, M_{N_R} . Notice that in the last line it was necessary to make explicit the mass arguments for the phase space of the jet momenta: $dL(l; q, M)$.

We define the approximation appropriate to the region R as a replacement symbolized by an operation T_R :

$$\begin{aligned}
\Gamma[W] \mapsto T_R \Gamma[W] &\equiv \int dL(\hat{l}; q, 0) H_R(\hat{l}, m \rightarrow 0) \\
&\times \prod_j \left[\int \frac{dM_j^2}{2\pi} \int dL(p_j; l_j, m) \Theta(M_j^2/\mu_F^2) J_{Rj}(p_j) \right] W(f). \tag{4.4}
\end{aligned}$$

This approximation is to be thought of as a kind of Taylor expansion of the hard part H_R . The hard subgraph and the associated phase-space integrations have been replaced by massless approximations, and \hat{l} is used to denote the massless approximated momenta that correspond to the incoming momenta of the jets. A precise definition of the relation between the approximated and unapproximated momenta will be given below. Note that the unapproximated jet momenta still have their physical non-zero invariant masses: $l_j^2 = M_j^2$.

In a region where the final-state lines of the subgraphs J_{Rj} do in fact form jets, $T_R \Gamma$ provides a good approximation to the original graph Γ , up to power-law corrections. However, we will need to use $T_R \Gamma$ outside the domain of validity of the approximation, and then the integrals over the jet masses M_j are no longer restricted by momentum conservation. It is therefore necessary to introduce a cut-off function $\Theta(M_j^2/\mu_F^2)$ for large jet masses. Here μ_F is the so-called ‘‘factorization scale’’, which in principle is arbitrary. The function $\Theta(x)$ must

equal one for small values of x and zero for large values of x , and for this an ordinary θ function is suitable⁶: $\Theta(x) = \theta(1 - x)$. However a smoother function would also be appropriate, and is likely to be better for numerical work [5].

The factorization scale determines the apportioning of the cross section between LO and NLO (and higher) corrections. As usual there is a renormalization-group invariance of the complete cross section under change of μ_F : When all orders of perturbation theory are included, the factorized cross section is accurate up to power-law corrections. However truncation of a perturbation expansion produces errors of the order of the next higher power of α_s , and an inappropriate choice of μ_F will produce logarithmically large perturbative corrections. For the hard scattering, μ_F should therefore be around Q , or a bit smaller, if the choice $\Theta(x) = \theta(1 - x)$ is made. This is because Q sets the typical scale for virtualities in a hard scattering. A change in the functional form of Θ simply corresponds to a more general renormalization-group transformation.

It may be useful to apply a constraint on μ_F so that the momenta automatically avoid violating the constraints given by momentum conservation. For this we choose μ_F so that $\Theta(M^2/\mu_F^2)$ is zero whenever $M > Q/N_R$, where N_R is the number of jet subgraphs for the region R .

B. Definition of projection onto massless momenta

The main element of the approximation $T_R\Gamma[W]$ in Eq. (4.4) is the replacement of the external momenta of H_R by a suitable massless and on-shell approximation; let us notate this by

$$\hat{l} = P_N(l). \quad (4.5)$$

The operator P_N is a kind of (non-linear) projection, and the definition⁷ that I choose is that in the overall center-of-mass frame

$$\begin{aligned} \hat{\mathbf{l}}_j &= \lambda^{-1} \mathbf{l}_j, \\ \hat{l}_j^0 &= |\hat{\mathbf{l}}_j|, \end{aligned} \quad (4.6)$$

with

$$\lambda = \sum_j |\mathbf{l}_j| / Q. \quad (4.7)$$

That is, the spatial momenta are simply scaled by a common factor λ so that the total spatial momentum remains zero. The scaling factor λ is chosen to give the correct total energy, so that the total energy-momentum is preserved:

$$\sum_j \hat{l}_j^\mu = \sum_j l_j^\mu = (Q, \mathbf{0}). \quad (4.8)$$

The physical requirement of conservation of energy and momentum has the mathematical consequence that the delta function $\delta^{(6)}(\sum_j l_j - q)$ in the phase-space integral remains unchanged, apart from a Jacobian factor, after the jet momenta l_j are replaced by their massless

⁶ Hence the notation!

⁷ It is likely that other definitions are possible and even useful. However, that issue will not be explored here.

approximations \hat{l}_j . Note also that the operator P_N satisfies the relation $P_N(P_N(l)) = P_N(l)$ characteristic of a projection.

The derivation of the factorization theorem will rely on the fact that the transformation $l \mapsto \hat{l}$ has a smooth limit when some or any of the masses of the momenta go to zero. This enables us to use an expansion in powers of masses relative to Q at appropriate places.

The inverse transformation from \hat{l} to l will be used in the Monte-Carlo algorithm. It is given by

$$\begin{aligned} \mathbf{l}_j &= \lambda \hat{\mathbf{l}}_j, \\ l_j^0 &= \sqrt{\mathbf{l}_j^2 + M_j^2}, \end{aligned} \quad (4.9)$$

with λ now being the solution of

$$\sum_j \sqrt{\lambda^2 \hat{\mathbf{l}}_j^2 + M_j^2} = Q. \quad (4.10)$$

Notice that this last equation has a solution if and only if $\sum_j M_j \leq Q$, and that then the solution is unique, with $0 \leq \lambda \leq 1$.

C. Jacobian

As we will see in later sections, a contribution to a hard scattering coefficient contains the value of an actual Feynman graph together with subtractions that prevent double counting of lower-order contributions. Internal lines in the original graph will have their exact energies and momenta, while the subtraction terms will have approximated energies and momenta. However, in a calculation of the hard scattering coefficient we must use the same phase-space measure in both the original graph and the subtractions. Therefore we will need the Jacobian of the transformation between the exact and the approximated parton momenta:

$$dL(\hat{l}; q, 0) = dL(l; q, M) \Delta(l), \quad (4.11)$$

so that, for example, Eq. (4.4) can be written as

$$\Gamma[W] \mapsto T_R \Gamma[W] \equiv \sum_f \Delta(l) H_R(\hat{l}, m=0) \prod_j \left[\Theta(l_j^2/\mu_F^2) J_{Rj}(p_j) \right] W(f), \quad (4.12)$$

where the sum over f means an integral over all final-states with the correct phase-space measure $dL(l; q, M)$, just as in Eq. (3.2).

Some reasonably straightforward manipulations show that the Jacobian is

$$\Delta(l) = \left(\prod_j \frac{l_j^0}{|\mathbf{l}_j|} \right) \sum_j \frac{\mathbf{l}_j^2}{l_j^0} \frac{\lambda^{5-4N_R}}{Q}. \quad (4.13)$$

Here again N_R is the number of jet subgraphs for the region in question, and λ is defined by Eq. (4.7). In a general number of space-time dimensions D , the formula remains the same, except that the factor of λ^{5-4N_R} is replaced by

$$\lambda^{D-1-(D-2)N_R}. \quad (4.14)$$

In the massless limit, the Jacobian approaches unity:

$$\Delta(l) = 1 + O(M^2/Q^2), \quad (4.15)$$

where the correction term contains a term for each of the masses.

In the case of a region with two jet subgraphs, $N_R = 2$, these formulae simplify, and we have

$$\lambda(2 \text{ jets}) = \frac{2|\mathbf{l}_1|}{Q} = \sqrt{\left[1 - \frac{(M_1 + M_2)^2}{Q^2}\right] \left[1 - \frac{(M_1 - M_2)^2}{Q^2}\right]}, \quad (4.16)$$

and

$$\Delta(2 \text{ jets}) = \left(\frac{Q}{2|\mathbf{l}_1|}\right)^3 = \left[1 - \frac{(M_1 + M_2)^2}{Q^2}\right]^{-3/2} \left[1 - \frac{(M_1 - M_2)^2}{Q^2}\right]^{-3/2}. \quad (4.17)$$

D. Jet factors and factorization

With the above definitions, we can rewrite the factorization formula Eq. (3.5) in terms of phase-space integrals for massless partons and of factorized integrals for each jet.

$$\sigma[W] = K \sum_{N=2}^{\infty} \int dL(\hat{l}; q, 0) \hat{H}_N \prod_j \left[\int \frac{dM_j^2}{2\pi} \int dL(p_j; l_j) \Theta(l_j^2/\mu_F^2) J_j(p_j) \right] W(f). \quad (4.18)$$

The use of the approximated phase-space measure, $dL(\hat{l}; q, 0)$, for the external lines of the hard scattering is important, since it keeps the algorithm in the event generator simple: the generation of the hard scattering part of the event can be performed without knowledge of the subsequent showering and hadronization of the external partons.

V. EXAMPLES

In this section, I will show how the methods used in the proof of the factorization theorem are applied to particular examples of Feynman graphs. This will provide detailed motivation for an appropriate construction of the contribution for each particular region of momentum space, and in particular for the form of the subtraction terms.

A. Need for subtractions

A initial attempt to obtain a factorization theorem goes as follows: First, sum Eq. (4.4) over all possible jet configurations. Then, for each configuration, sum over all possible graphs compatible with the configuration. As follows from the argument in Sec. III C, the result would appear to have the factorized form given in Eq. (3.5) or (4.18), provided that we define the contribution associated with region R to be

$$C_R \Gamma(\text{region method}) = T_R \Gamma \Big|_{\text{restricted to region } R}. \quad (5.1)$$

We would then define the hard scattering coefficient \hat{H}_N to be simply the sum over all graphs that make N massless outgoing partons, but with a restriction on the momenta to be in the

appropriate hard region. There is a corresponding restriction to collinear configurations in the jet factor.

Although this simple phase-space-slicing argument contains a core of truth, it fails to be exactly correct, for several interrelated reasons:

- The boundaries of the various regions are hard to define precisely for the general case, and most importantly the regions are liable not to factorize into hard and collinear parts.
- If one does require a factorized form for the shapes of the regions in momentum space, it is possible that there can be double counting of some parts of momentum space, and omissions of other parts. It is quite unobvious how to automatically avoid such double- and/or non-counting in general, with a phase-space-slicing method.
- A particular jet subgraph may correctly lie just below a threshold defining a jet, but some lines in the hard part may have invariant masses only just above the threshold. Then it is far from clear that the massless approximation for the external lines of the hard part results in a power-suppressed error. So there is a danger that the factorization theorem proved with the phase-space-slicing method fails to accomplish its purpose of providing an approximation to the cross section that is valid to the whole leading power.

Instead, we will use a subtractive method. We will still construct the asymptotic form of the cross section as a sum over terms, one for each region of each graph, as in Eqs. (3.3) and (3.4). Each term $C_R(\Gamma)$ will be exactly a contribution to the hard scattering times a contribution to the jet factors, and it will also equal the basic approximation $T_R\Gamma$ plus subtraction terms that cancel the effects of double counting between regions. However, the use of a subtraction method allows the integrals over momentum to be unrestricted. The sum over all graphs and regions then gives the factorization formula, Eq. (3.5). The combinatoric argument is the same as in the naive phase-space slicing method, but now there is no restriction on the integrations, other than from the cut-off function Θ in the definition of the jet factor—see Eq. (4.18) and Eq. (6.42) below.

B. Simple example

In this section, I will implement the subtraction method for the simplest example, the cut graph, A , of Fig. 2, whose final state has three particles, of momenta p_1 , p_2 and p_3 . I will give a lot of explicit detail for what is actually a fairly simple problem. The reason is that the techniques will generalize to much more complicated situations, but only a precise treatment will make this generalization clear.

The graph has the following regions for its leading twist contributions:

R_1 : p_1 and p_2 are almost parallel.

R_2 : All the final-state momenta are at wide angles with respect to each other. This is a purely ultra-violet region where the graph can be correctly approximated by setting all masses to zero.

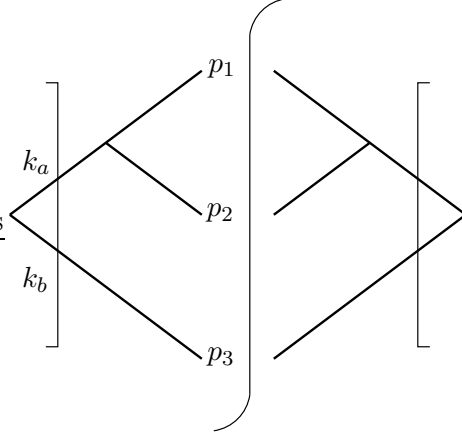


FIG. 6: First leading region of Fig. 2, and its standard approximation. The vertical bars with the squared ends indicate where the collinear approximation of Eq. (4.4) is made.

We will see how, in the leading power of Q , Γ can be written as a sum of a term for each of the two regions, plus a suppressed remainder term:

$$A = A_1 + A_2 + O\left(|A| \frac{m^2}{Q^2}\right). \quad (5.2)$$

Here, each of A_1 and A_2 is a particular term on the right-hand side of Eq. (3.3), with A_j meaning $C_{R_j}(A)$.

Region R_1 In this region, a good approximation, symbolized in Fig. 6, is

$$A_1 \equiv T_{R_1} \Gamma = dL(k_a, k_b; q, 0) H_{A_1}(k_a, k_b) dD_{12}(p_1, p_2), \quad (5.3)$$

where I have used the definition, Eq. (4.4), for the Taylor expansion operator, T_{R_1} .

In this approximation the two external momenta of the hard subgraph are replaced by on-shell massless momenta:

$$k_a^\mu = \frac{(|\mathbf{p}_1 + \mathbf{p}_2|, \mathbf{p}_1 + \mathbf{p}_2)}{\lambda_{A_1}} = \frac{Q}{2} (1, -\mathbf{p}_3/|\mathbf{p}_3|), \quad (5.4)$$

$$k_b^\mu = \frac{Q}{2} (1, \mathbf{p}_3/|\mathbf{p}_3|). \quad (5.5)$$

The scaling parameter λ_{A_1} that appears in the transformation between the exact jet momenta and the massless approximation has the value

$$\lambda_{A_1} = \frac{2|\mathbf{p}_3|}{Q}. \quad (5.6)$$

In the projection notation, $(k_a, k_b) = P_2(p_1 + p_2, p_3)$.

The hard scattering factor in Eq. (5.3) is simply unity, which is the value of the lowest order graph. The jet factor is defined by a suitable specialization of the factor in square brackets in Eq. (4.18):

$$dD_{12} = \int \frac{dM_{12}^2}{2\pi} dL(p_1, p_2; l_{12}) \Theta(M_{12}^2/\mu_F^2) \frac{g^2}{[(p_1 + p_2)^2 - m^2]^2}. \quad (5.7)$$

Here, $l_{12}^\mu \equiv p_1^\mu + p_2^\mu$ is the exact momentum of the intermediate parton. The errors in the approximation are solely in the massless approximation to the two-particle phase space, so that we can write

$$A = A_1 \left[1 + O(M_{12}^2/Q^2) \right]. \quad (5.8)$$

Here M_{12} is the invariant mass of the final state in the jet subgraph, i.e., $\sqrt{(p_1 + p_2)^2}$.

When we construct the subtractions for the second region, we will need the formula for the approximation in terms of the original phase-space integration:

$$A_1 = dL(p; q, m) \Delta_{A1} \Theta((p_1 + p_2)^2/\mu_F^2) \frac{g^2}{[(p_1 + p_2)^2 - m^2]^2}, \quad (5.9)$$

where the Jacobian is

$$\Delta_{A1} = \left(\frac{Q}{2|\mathbf{p}_3|} \right)^3, \quad (5.10)$$

from Eq. (4.17).

Region R_2 In this region, all the external particles are at wide angle, so that the appropriate approximation to the whole graph is

$$T_{R_2} A = dL(l_{2,a}, l_{2,b}, l_{2,c}; q, 0) H_{A2}(l_{2,a}, l_{2,b}, l_{2,c}). \quad (5.11)$$

The hard subgraph H_{A2} is the whole graph, taken in the massless approximation:

$$H_{A2} = \frac{g^2}{[(l_{2,a} + l_{2,b})^2]^2}, \quad (5.12)$$

and its external momenta are:

$$l_{2,a}^\mu = \frac{(|\mathbf{p}_1|, \mathbf{p}_1)}{\lambda_{A2}}, \quad (5.13)$$

$$l_{2,b}^\mu = \frac{(|\mathbf{p}_2|, \mathbf{p}_2)}{\lambda_{A2}}, \quad (5.14)$$

$$l_{2,c}^\mu = \frac{(|\mathbf{p}_3|, \mathbf{p}_3)}{\lambda_{A2}}, \quad (5.15)$$

where

$$\lambda_{A2} = \frac{|\mathbf{p}_1| + |\mathbf{p}_2| + |\mathbf{p}_3|}{Q} = 1 + O(m^2/Q^2). \quad (5.16)$$

Now we note two related facts

- H_{A2} has a collinear singularity when $l_{2,a}$ and $l_{2,b}$ become parallel.
- Term A_1 , which I have constructed to be a good approximation in region R_1 , also contributes in the larger region R_2 .

So I define A_2 by approximating the original graph minus the approximation I have already constructed for the smaller region R_1 . The simplest definition would be $A_2 = T_{R_2}(A - T_{R_1}A)$. However a small modification turns out to be convenient, and I define

$$\begin{aligned} A_2 &= V(\widetilde{M}_{12}/m) T_{R_2}(A - T_{R_1}A) \\ &= dL(p; q) V(\widetilde{M}_{12}/m) \Delta_{A_2} \frac{g^2}{[(l_{2,a} + l_{2,b})^2]^2} \left[1 - \Theta((l_{2,a}^2 + l_{2,b}^2)/\mu_F^2) \Delta_{A_1'} \right]. \end{aligned} \quad (5.17)$$

Here Δ_{A_2} is the Jacobian for the transformation $(p_1, p_2, p_3) \mapsto (l_{2,a}, l_{2,b}, l_{2,c})$, which is equal to unity plus corrections of order m^2/Q^2 . The Jacobian $\Delta_{A_1'}$ in the subtraction term is the approximation to Δ_{A_1} in which the momenta p_1 , etc., are replaced by their massless approximations $l_{2,a}$, etc., i.e.,

$$\Delta_{A_1'} = \left(\frac{Q}{2|l_{2,c}|} \right)^3 = \Delta_{A_1} \times \left[1 + O(m^2/Q^2) \right], \quad (5.18)$$

The remaining factor $V(\widetilde{M}_{12}, m)$ is what I will call a ‘‘collinear veto factor’’. Its purpose is to remove a spurious collinear divergence. After explaining the need for this factor, I will show that the sum of A_1 and A_2 provides a good approximation everywhere, Eq. (5.2).

First, recall that A_1 is obtained from A by the approximation of neglecting both the jet mass M_{12} and the particle masses with respect to Q . So the sources of error give terms of order M_{12}^2/Q^2 or m^2/Q^2 . Since M_{12} is always larger than $2m$, we can write

$$A - A_1 = O\left(|A| \frac{M_{12}^2}{Q^2}\right). \quad (5.19)$$

We need to assume here that the factorization scale μ_F is of order Q ; otherwise we would have a large logarithmic contribution to the total cross section.

Next, we observe that A_2 is obtained from $A - A_1$ by applying a massless approximation for the external particles, as is appropriate when all the particles are at wide angles. This approximation results in an approximated jet mass \widetilde{M}_{12} that is different from M_{12} . When the final-state particles are at wide angles, the exact and approximated masses are equal up to corrections of relative size m^2/Q^2 . But as the two particles become exactly parallel, the approximated jet mass goes to zero and produces a singularity in the propagator denominator, whereas the exact jet mass never goes below $2m$. Thus, without the veto factor, A_2 has a singularity in the collinear region. Indeed, when we replace the correct propagators $1/[(p_1 + p_2)^2 - m^2]^2$ in the original graph A by their massless approximation $1/[(l_{2,a} + l_{2,b})^2]^2$, we get a well-known logarithmic collinear divergence in the integral over all jet masses.

However, the estimate Eq. (5.19) ensures that there is a power-law suppression:

$$\begin{aligned} A_2 &= O\left(|A - A_1| \frac{m^4}{\widetilde{M}_{12}^4}\right) \\ &= O\left(|A| \frac{\widetilde{M}_{12}^2}{Q^2} \frac{m^4}{\widetilde{M}_{12}^4}\right) \\ &= O\left(|A(m=0)| \frac{\widetilde{M}_{12}^2}{Q^2}\right). \end{aligned} \quad (5.20)$$

The estimate on the first line results from the replacement of the exact propagator by the massless approximation, and is valid when $\widetilde{M}_{12} \lesssim m$. The second line results from applying Eq. (5.19) in the massless approximation.

Although we now see that the logarithmic divergence in the integrated cross section has been removed, there remains a divergence in the differential cross section. This can be quite annoying in practice, and it also complicates the proofs and error estimates. So we simply remove the divergence by defining A_2 to include a veto factor $V(\widetilde{M}_{12}/m)$. One suitable veto factor is simply a theta function

$$V(\widetilde{M}_{12}/m) = \theta(\widetilde{M}_{12} - 2m). \quad (5.21)$$

Any other function satisfying the following properties would be equally good:

- V is zero when \widetilde{M}_{12} is significantly less than m .
- V is unity when \widetilde{M}_{12} is significantly greater than m .

The first requirement ensures that the divergences are removed. Indeed the whole region when A_2 is much larger than $A - A_1$ is also removed, i.e., the region where a massless approximation to $A - A_1$ is a disaster. Since the purpose of A_2 is to handle momentum configurations far from the collinear region, the precise functional form of V in the collinear region is irrelevant to physics. The second requirement, that V be unity away from the collinear region, ensures that A_2 accomplishes its purpose of participating in a better approximation to A in the non-collinear region, R_2 .

The veto factor ensures that the approximated jet mass \widetilde{M}_{12} is never much smaller than m , i.e., $\widetilde{M}_{12} \gtrsim m$. In this case, the true and approximated jet masses are comparable. Thus, when we set m to zero in calculating A_2 , we are neglecting m in comparison with the smallest virtuality, which is always of order M_{12} . Hence

$$A_2 - (A - A_1) = O\left(\frac{m^2}{M_{12}^2} |A - A_1|\right) = O\left(\frac{m^2}{Q^2} |A|\right), \quad (5.22)$$

where we have used Eq. (5.19). This is exactly the desired result, Eq. (5.2).

Notice how the exact form of the veto factor does not affect this derivation. A change in the veto factor only affects the collinear region, $M_{12} \sim m$. Although the change might result in a 100% change in A_2 , this does not affect the error estimate, since both $A - A_1$ and A_2 are inevitably of order m^2/Q^2 (relative to A) in this region.

C. Harder example

In this section, we treat a more complicated example, the cut graph, Γ , of Fig. 4, which has four particles in the final state, of momenta p_1 , p_2 , p_3 and p_4 . As was observed earlier, the graph has the following regions for leading twist contributions:

R_1 : p_1 and p_2 are almost parallel, and p_3 and p_4 are also almost parallel.

R_2 : p_3 and p_4 are almost parallel, but p_1 and p_2 are at wide angle.

R_3 : p_1 and p_2 are almost parallel, but p_3 and p_4 are at wide angle.

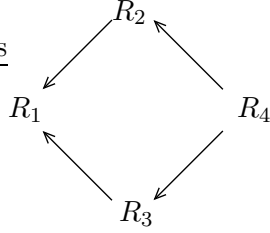
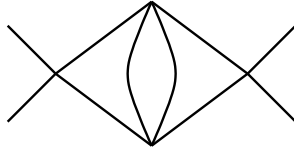


FIG. 7: Relation between leading regions of Fig. 4.

FIG. 8: Graph in ϕ^4 theory with overlapping ultra-violet divergences.

R_4 : All the final-state momenta are at wide angles with respect to each other.

Our treatment will start off being almost identical to that for Fig. 2, in Sec. VB. But complications will arise later because there is the equivalent of an overlapping divergence.

As before, I will show how, in the leading power of Q , Γ can be written as the sum of a term for each of the four regions, plus a suppressed remainder term:

$$\Gamma = \Gamma_1 + \Gamma_2 + \Gamma_3 + \Gamma_4 + O\left(|\Gamma| \frac{m^2}{Q^2}\right). \quad (5.23)$$

In the more general notation of Eq. (3.3), we would have $C_{R_1}\Gamma$ instead of Γ_1 , etc. To organize the subtractions in these terms, we need an ordering relation between the regions, which is essentially set theoretic inclusion. For the graph under discussion, this relation is symbolized in Fig. 7, and I notate the corresponding orderings as $R_1 < R_2$, $R_1 < R_3$, $R_2 < R_4$ and $R_3 < R_4$. This means that R_1 is contained in both R_2 and R_3 , and that both R_2 and R_3 are contained in R_4 . This same structure appears in simple examples of overlapping ultra-violet divergences. (For example it gives the relationships between the regions of UV divergence for the graph of Fig. 8.) Thus the example of Fig. 4 provides an interesting and non-trivial test of our methods.

A general and precise definition of the ordering is made by associating each region with a particular set of momentum configurations of massless momenta, and then defining the ordering as simple set theoretic inclusion of these massless configurations. The configurations associated with a region R are those where the momenta within each jet are made massless and exactly parallel. These are exactly the configurations that are used to classify the pinch singularities of massless graphs in the Libby-Sterman analysis [10]. For example, the configurations for R_1 are all those for which p_1 and p_2 are exactly parallel and massless and p_3 and p_4 are exactly parallel and massless. Similarly, the configurations for R_2 are those for which p_3 and p_4 are exactly parallel. Thus one set of momenta is contained in the other: $R_1 \subset R_2$, and I use this as the definition⁸ of $R_1 < R_2$.

⁸ Note carefully the distinction between the massless collinear configurations that are used to define relations like $R_1 < R_2$ and the corresponding sets of momenta that give the important regions contributing to the

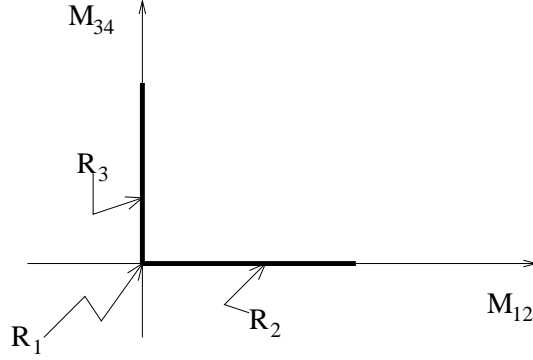


FIG. 9: Geometry of the leading regions for Fig. 4.

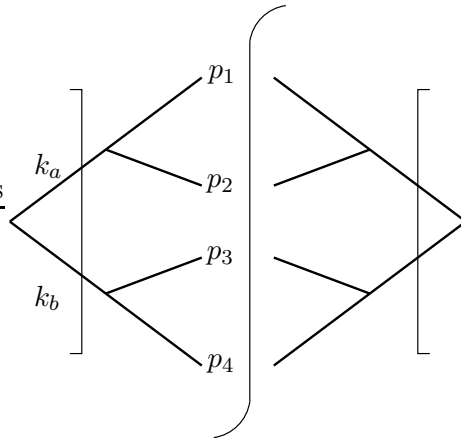


FIG. 10: First leading region of Fig. 4, and its standard approximation.

In the case of the regions for our graph, a convenient visualization of the geometry is given in Fig. 9. This shows the plane of the two relevant variables, the mass M_{12} of the (12) pair and the mass M_{34} of the (34) pair. The singular surface associated with R_1 is

cross section. The massless collinear configurations form skeletons, so to speak, for the regions. Defining the relations $R_1 < R_2$ by set-theoretic inclusion for the skeletons is exactly literally correct. But the same definition applied to the regions requires careful interpretation to deal with the boundaries etc. (The concept of a massless collinear momentum configuration is precisely defined, but the concept of an important momentum region is rather fuzzy and not susceptible to a precise and useful mathematical definition.)

A related issue is the commonly seen misunderstanding that the factorization theorem is concerned with the contributions of collinear (and soft) divergences. Literally speaking, this assertion is false, as is clear in any field theory that has non-zero masses for all its fields: these preclude there from being actual collinear and soft divergences, even though the factorization theorem remains valid. It is true that the leading contributions are *associated* with divergences. But the divergences are not necessarily literally present in the actual theory, and a correct treatment cannot assume this. The correct statement is that leading regions of momentum space can be labeled by the skeleton configurations that are surfaces of pinch singularities in massless Feynman graphs, and that the leading regions are contained in neighborhoods of the skeleton configurations.

the point $M_{12} = M_{34} = 0$; the surface associated with R_2 is the line $M_{34} = 0$, restricted to the physically accessible region; the surface associated with R_3 is the line $M_{12} = 0$, again restricted to the physically accessible region; and the ultra-violet region R_4 is the whole plane. Set theoretic relations between these sets of points evidently give $R_1 < R_2$, $R_1 < R_3$, $R_2 < R_4$ and $R_3 < R_4$.

The construction of Eq. (5.23) will use this ordering. I will start with the smallest region, R_1 , and construct its term Γ_1 to be a good approximation to Γ in this region. Then I will successively construct the terms for larger regions. Each term will be arranged so that, when added to the previously constructed terms, it does not violate the validity of the approximations provided by these terms. The first part of the treatment is therefore very close to that of the lower-order graph Fig. 2.

From the Feynman rules of the theory, we see that the contribution of the unapproximated graph to the cross section is (up to overall kinematic factors):

$$\Gamma = dL(p; q, m) \frac{g^4}{[(p_1 + p_2)^2 - m^2]^2 [(p_3 + p_4)^2 - m^2]^2}. \quad (5.24)$$

Region R_1 In this region, a good approximation, symbolized in Fig. 10, is

$$\Gamma_1 \equiv T_{R_1} \Gamma = dL(k_a, k_b; q, 0) H_1(k_a, k_b) dD_{12}(p_1, p_2) dD_{34}(p_3, p_4). \quad (5.25)$$

It is the obvious generalization of A_1 , in Eq. (5.3), and it is again constructed by replacing the external momenta of the hard subgraph by on-shell massless momenta, which are now

$$\begin{aligned} k_a^\mu &= \lambda_1^{-1}(|\mathbf{p}_1 + \mathbf{p}_2|, \mathbf{p}_1 + \mathbf{p}_2) \\ &= \frac{Q}{2} \left(1, \frac{\mathbf{p}_1 + \mathbf{p}_2}{|\mathbf{p}_1 + \mathbf{p}_2|} \right), \end{aligned} \quad (5.26)$$

$$\begin{aligned} k_b^\mu &= \lambda_1^{-1}(|\mathbf{p}_3 + \mathbf{p}_4|, \mathbf{p}_3 + \mathbf{p}_4) \\ &= \frac{Q}{2} \left(1, -\frac{\mathbf{p}_1 + \mathbf{p}_2}{|\mathbf{p}_2 + \mathbf{p}_2|} \right). \end{aligned} \quad (5.27)$$

Here

$$\lambda_1 = \frac{2|\mathbf{p}_1 + \mathbf{p}_2|}{Q}. \quad (5.28)$$

In the projection notation, $(k_a, k_b) = P_2(p_1 + p_2, p_3 + p_4)$.

The hard scattering factor H_1 in Eq. (5.25) is simply unity, which is the value of the lowest order graph. The jet factors are defined by Eq. (5.7) for dD_{12} , and a corresponding formula for dD_{34} . The errors in the approximation are solely in the massless approximation to the phase space of the hard scattering. Therefore we have

$$\Gamma = \Gamma_1 \left[1 + O(M_1^2/Q^2) \right], \quad (5.29)$$

where M_1 is the larger of the masses of the two pairs of particles: $M_1^2 = \max(M_{12}^2, M_{34}^2)$.

In constructing subtractions for other regions, we will need the formula for the approximation in terms of the original phase-space integration:

$$\Gamma_1 = dL(p; q, m) \Delta_1 \frac{g^2 \Theta((p_1 + p_2)^2 / \mu_F^2)}{[(p_1 + p_2)^2 - m^2]^2} \frac{g^2 \Theta((p_3 + p_4)^2 / \mu_F^2)}{[(p_3 + p_4)^2 - m^2]^2}, \quad (5.30)$$

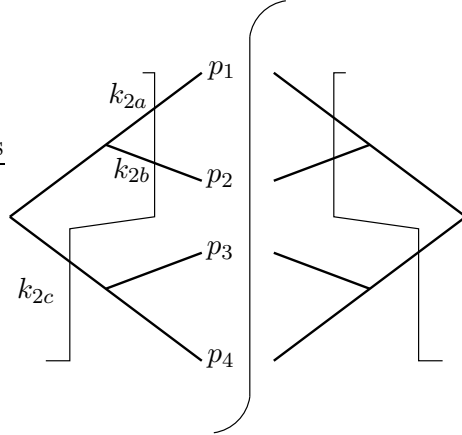


FIG. 11: Second leading region of Fig. 4 and its standard approximation.

where the Jacobian is

$$\Delta_1 = \left(\frac{Q}{2|\mathbf{p}_1 + \mathbf{p}_2|} \right)^3, \quad (5.31)$$

from Eq. (4.17).

Observe that Γ_1 differs from the original graph only by the Jacobian of the phase space and by the cut-offs for the jet factors. So in terms of methods for calculating individual low-order Feynman graphs, we have gained nothing; indeed we have lost something. What we have gained is a form that can be generalized to higher-order graphs and converted to a systematic algorithm for obtaining useful approximations to large numbers of graphs with a computational effort merely proportional to the number of final-state particles.

Region R_2 In this region, where only particles 3 and 4 are collinear, the appropriate approximation to the whole graph is symbolized in Fig. 11:

$$T_{R_2}\Gamma = dL(k_{2,a}, k_{2,b}, k_{2,c}; q, 0) H_2(k_{2,a}, k_{2,b}, k_{2,c}) dD_{34}(p_3, p_4). \quad (5.32)$$

The hard part H_2 is (the square of) the left-hand subgraph of Fig. 11:

$$H_2 = \frac{g^2}{[(k_{2,a} + k_{2,b})^2]^2}, \quad (5.33)$$

whose external momenta are on-shell and massless:

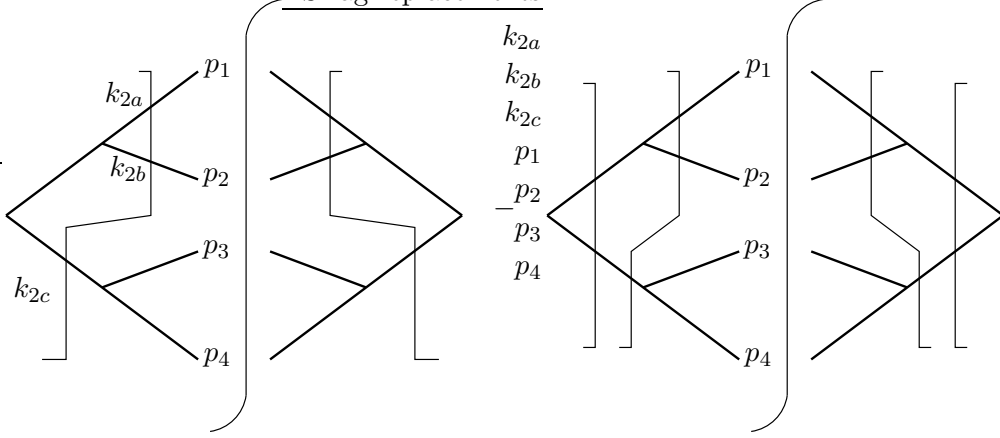
$$k_{2,a}^\mu = \lambda_2^{-1}(|\mathbf{p}_1|, \mathbf{p}_1), \quad (5.34)$$

$$k_{2,b}^\mu = \lambda_2^{-1}(|\mathbf{p}_2|, \mathbf{p}_2), \quad (5.35)$$

$$k_{2,c}^\mu = \lambda_2^{-1}(|\mathbf{p}_3 + \mathbf{p}_4|, \mathbf{p}_3 + \mathbf{p}_4), \quad (5.36)$$

where

$$\lambda_2 = \frac{|\mathbf{p}_1| + |\mathbf{p}_2| + |\mathbf{p}_3 + \mathbf{p}_4|}{Q}. \quad (5.37)$$

FIG. 12: Definition of Γ_2 .

Just as before, I define the contribution associated with region R_2 by subtracting an allowance for the smaller region R_1 :

$$\begin{aligned}
\Gamma_2 &= V_2 T_{R_2}(\Gamma - \Gamma_1) \\
&= V_2 T_{R_2}(\Gamma - T_{R_1}\Gamma) \\
&= dL(p; q) \Delta_2 V_2 \frac{g^2 \Theta((p_3^2 + p_4^2)/\mu_F^2)}{[(p_3 + p_4)^2 - m^2]^2} \frac{g^2}{[(k_{2,a} + k_{2,b})^2]^2} \times \\
&\quad \times \left[1 - \Theta((k_{2,a}^2 + k_{2,b}^2)/\mu_F^2) \Delta_{1'} \right]. \tag{5.38}
\end{aligned}$$

Here

- The Jacobian for the transformation to $k_{2,a}$, $k_{2,b}$, and $k_{2,c}$ is

$$\Delta_2 = \frac{E_1}{|\mathbf{p}_1|} \frac{E_2}{|\mathbf{p}_2|} \frac{E_3 + E_4}{|\mathbf{p}_3 + \mathbf{p}_4|} \left(\frac{\mathbf{p}_1^2}{E_1} + \frac{\mathbf{p}_2^2}{E_2} + \frac{(\mathbf{p}_3 + \mathbf{p}_4)^2}{E_3 + E_4} \right) \frac{1}{\lambda_2^7 Q}, \tag{5.39}$$

from Eq. (4.13).

- $\Delta_{1'}$ is Δ_1 with the momenta $\mathbf{p}_1 + \mathbf{p}_2$ and $\mathbf{p}_3 + \mathbf{p}_4$ replaced by $\mathbf{k}_{2,a} + \mathbf{k}_{2,b}$ and $\mathbf{k}_{2,c}$, i.e.,

$$\Delta_{1'} = \left(\frac{Q}{2|\mathbf{k}_{2,c}|} \right)^3. \tag{5.40}$$

- The veto factor V_2 is defined to be

$$V_2 = V(\widetilde{M}_{12}/m), \tag{5.41}$$

where V is the same veto function as in Eq. (5.21). The reason for requiring a veto factor is the same as with Eq. (5.17).

The formula for Γ_2 is symbolized in Fig. 12. It is power suppressed in the smaller region R_1 , whereas the massless approximations to the individual terms Γ and Γ_1 both have collinear

singularities on the surface R_1 . The sum of the two terms I have generated so far gives a good approximation to the original graph in a neighborhood of R_2 (and hence of the smaller surface R_1 , whose defining surface is a subsurface of R_2):

$$\Gamma = (\Gamma_1 + \Gamma_2) \left[1 + O(M_{34}^2/Q^2) \right], \quad (5.42)$$

where M_{34} is the mass of the pair of particles 3 and 4. The proof of this equation is the same as for the corresponding equation Eq. (5.2) for the simpler graph.

A quick examination of Fig. 9 might suggest that there is some kind of singularity on the line R_3 , and that this would cause a problem in applying the above argument around the point R_1 . This is not so. The treatment of the double-collinear region associated with R_1 applies uniformly in a whole neighborhood of the point R_1 . The line R_3 gains its significance only when one moves substantially away from R_1 and finds a region where only p_1 and p_2 are collinear while the other momenta are at wide angles.

There is an important transitivity property of successive projections of momenta. We obtained k_a and k_b by a projection of the four momenta p_1, p_2, p_3 and p_4 . Instead we could project the three momenta $k_{2,a}, k_{2,b}$, and $k_{2,c}$ onto two momenta by

$$k_{a'}^\mu = \lambda_{21}^{-1} \left(|\mathbf{k}_{2a} + \mathbf{k}_{2b}|, \mathbf{k}_{2a} + \mathbf{k}_{2b} \right), \quad (5.43)$$

$$k_{b'}^\mu = \lambda_{21}^{-1} \left(|\mathbf{k}_{2,c}|, \mathbf{k}_{2,c} \right), \quad (5.44)$$

with

$$\lambda_{21} = \frac{|\mathbf{k}_{2a} + \mathbf{k}_{2b}| + |\mathbf{k}_{2,c}|}{Q}. \quad (5.45)$$

It is readily verified that $k_{a'}^\mu = k_a^\mu$ and $k_{b'}^\mu = k_b^\mu$. This is the transitivity property: one gets the same momenta by any appropriate sequence of projections. The proof in general is made by observing that each projection amounts to scaling all the relevant spatial momenta by a factor. The energies are defined by requiring the particles to be massless, and the scaling factor is defined by requiring the total energy always to be Q .

Region R_3 Just as with region R_2 , I define

$$\Gamma_3 = V_3 T_{R_3}(\Gamma - \Gamma_1), \quad (5.46)$$

and I add it to the list of previously generated terms to obtain $\Gamma_1 + \Gamma_2 + \Gamma_3$.

But now a new problem appears when we try to show that $\Gamma_1 + \Gamma_2 + \Gamma_3$ is equal to Γ up to a non-leading term near *both* the singular surfaces R_2 and R_3 . We have already seen that the sum of two of the terms, $\Gamma_1 + \Gamma_2$, is close to Γ near R_2 — see Eq. (5.42). Of course, it is also true that the sum of the other pair of terms, $\Gamma_1 + \Gamma_3$, is close to Γ near R_3 . But what we need is a result for the sum of all three terms. This extra complication is associated with the “overlapping divergence” structure in the relations between the regions, as symbolized in Figs. 7 and 9.

What we need to show is that the sum of the three terms is a good approximation in a neighborhood of both R_2 and R_3 (and of R_1), i.e.,

$$\Gamma = (\Gamma_1 + \Gamma_2 + \Gamma_3) \left[1 + O(M^2/Q^2) \right], \quad (5.47)$$

where now M is the minimum of: (a) the mass of the pair of particles 1 and 2, and (b) the mass of the pair of particles 3 and 4.

The arguments I have used are sufficient provided that I prove the additional results

- Γ_2 is power suppressed in region R_3 : it is $O(\Gamma M_{12}^2/Q^2)$.
- Γ_3 is power suppressed in region R_2 : it is $O(\Gamma M_{34}^2/Q^2)$.

These can be summarized by saying that each term is power-suppressed when we approach a region that overlaps the design region of the given term.

Consider first Γ_2 , whose definition is given in Fig. 12, or equivalently Eq. (5.38). It is designed with region R_2 in mind, which is the region where the lower two external lines (p_3 and p_4) are collinear. That is, it is concerned with a neighborhood of the line labeled R_2 in Fig. 9. Now Γ_2 contains a subtraction which cancels the leading contribution from the smaller region R_1 . That is, there is a power suppression, $O(M_{12}^2/Q^2)$ relative to the size of Γ , when the upper two external lines become collinear. This suppression appears as one moves along the horizontal line in Fig. 9.

Now observe that this suppression holds over the whole region of phase space, rather than just only around R_2 , the horizontal axis in Fig. 9. The reason is simply that in the definition Fig. 12 of Γ_2 , the dependence on M_{34} is completely factored out. The cancellation that gives the $O(M_{12}^2/Q^2)$ estimate works independently of the value of M_{34} , i.e., independently of whether the (34) pair is collinear. To put it another way, the application of the T_{R_2} operation has put the k_{2c} line in Fig. 9 exactly massless and on-shell, so it is as if the (34) pair were exactly collinear.

We therefore find that

$$\Gamma_2/\Gamma = O(M_{12}^2/Q^2). \quad (5.48)$$

Observe that when we integrate Γ_2 over all final states, the power law suppression is worsened by a logarithm that arises from the integral over the mass of the (3,4) pair.

The construction of Γ_3 is precisely such that $\Gamma_1 + \Gamma_3$ gives a good approximation to Γ when (12) are collinear, i.e., when M_{12} is small. Hence $\Gamma = (\Gamma_1 + \Gamma_2 + \Gamma_3)[1 + O(M_{12}^2/Q^2)]$.

Exactly similarly, Γ_3 is proved to be suppressed in region R_2 , and so $\Gamma = (\Gamma_1 + \Gamma_2 + \Gamma_3)[1 + O(M_{34}^2/Q^2)]$. We have two error estimates that are both valid, so the strongest provides the best estimate, which is Eq. (5.47).

These new results, as well as the suppression of Γ_2 and Γ_3 in region R_1 , are specific examples of a general result, to be proved later in full generality:

For any graph Γ and any of its regions R , $C_R(\Gamma)$ is power suppressed in neighborhoods of all regions R' except those for which $R' \geq R$.

Thus $C_R(\Gamma)$ gives a leading contribution in R itself, as it should, and in bigger regions. Its very construction ensures that it is suppressed in smaller regions. We have now seen in an example that it is also suppressed in other regions R' that merely intersect with R (or do not intersect it at all).

Region R_4 The contribution associated with the purely ultra-violet region can now be constructed as

$$\Gamma_4 = V_4 T_{R_4}(\Gamma - \Gamma_1 - \Gamma_2 - \Gamma_3). \quad (5.49)$$

The veto factor must cut out both of the extreme collinear regions, and we can define it as

$$V_4 = V(\widetilde{M}_{12}/m) V(\widetilde{M}_{34}/m), \quad (5.50)$$

where V is the elementary veto function defined in Eq. (5.21).

Sum With the use of all the results I have derived, it is easy to show that the sum of all the terms $\Gamma_1 + \Gamma_2 + \Gamma_3 + \Gamma_4$ gives a good approximation to Γ in all the regions, so that we obtain Eq. (5.23). Observe that all these cancellations work point by point in the momenta of the final-state particles. Thus they happen independently of the weighting function W , and thus independently of which cross section we wish to compute. This is in contrast to the “analytic” methods of calculation in perturbative QCD, which treat the subtractions as delta functions. In the analytic methods, the power suppression of the error only occurs after an integral over final states with a collinear-safe weight function.

VI. PROOF OF FACTORIZATION

In this section, I will give the actual proof of the factorization theorem. The theorem is of a form that allows the construction of a corresponding Monte-Carlo algorithm in Sec. VII. As is usual in such proofs, the details can be tedious to work through unless one has a clear overall view of the ideas and aims. These are all based on experience with the examples presented earlier.

So first, in Sec. VIA, I will give an overall view: One starts from the characterization of the possible regions that are important, and then defines corresponding contributions with subtractions to prevent double counting. These individual contributions are of such a form that summing over all possibilities gives a suitable factorization formula.

The subsequent technical work is to show mathematically that the subtraction terms do indeed perform the job that they are constructed to perform. This is done by constructing suitable estimates of graphs and subgraphs before and after subtraction.

A. Overall view

As we have already seen, the leading regions for graphs are characterized by a decomposition into subgraphs: a hard subgraph where all the internal momenta are highly virtual, and two or more jet subgraphs. So for a leading region R of a graph Γ , we can symbolize the decomposition as

$$H_R \times J_{R1} \cdots \times J_{RN_R}, \quad (6.1)$$

where N_R is the number of jet subgraphs for the region. Analytically, the region is a neighborhood of a particular pinch-singular surface (PSS), as shown by Libby and Sterman [10], and the decomposition into subgraphs corresponds to a factorization of the integrand.

For each leading region we construct an approximation to the integrand by applying a suitable Taylor expansion to the hard subgraph:

$$T_R\Gamma = T_R(H_R) \times J_{R1} \cdots \times J_{RN_R}, \quad (6.2)$$

Just as in the examples, the Taylor expansion is used to approximate the hard subgraph by a massless on-shell partonic quantity and hence to correctly approximate the momentum integrals by a suitable factorizable form. This is what enables convenient calculations to be done: after the summation over graphs, the hard subgraph can be calculated independently of the hadronization of the produced partons.

As we saw, we must avoid double counting, so the contribution for leading region R is obtained by applying the above manipulations not to the original graph but to the original

graph minus the previously constructed terms for smaller leading regions. In addition, we found it convenient to insert a veto factor that excludes small neighborhoods of the massless collinear configurations of the Taylor-expanded hard subgraph. So we define

$$C_R(\Gamma) = V_R T_R \left(\Gamma - \sum_{R' < R} C_{R'} \Gamma \right). \quad (6.3)$$

This equation gives a recursive definition of the contribution $C_R(\Gamma)$ for region R , since it involves only the same quantity for smaller regions. The recursion starts with the minimal region(s) R_{\min} , i.e., those that contain no smaller regions. For these

$$C_{R_{\min}} \Gamma = T_{R_{\min}} \Gamma. \quad (6.4)$$

Hence Eq. (6.3) is a valid definition of C_R .

The veto factor can be defined as a product of an elementary veto functions:

$$V_R = \prod_j V(\widetilde{M}_j/m). \quad (6.5)$$

Here the product is over all combinations of external lines of the hard subgraph of R , and \widetilde{M}_j is the invariant mass of these lines in the massless approximation. The elementary veto function V is defined in Eq. (5.21). Although there is an arbitrariness in the choice of the veto factors, the precise choice will not affect the physics, as we have already observed,

Now follows a very critical point. The double-counting subtractions are applied on smaller leading regions than R and thus to leading regions whose hard subgraph is strictly smaller than H_R . Moreover the Taylor expansions are always applied to the hard subgraphs, with the jet factors being left completely unaltered, as is appropriate for quantities that are ultimately to be regarded as unknown non-perturbative quantities. Hence the subtractions are applied inside the hard subgraph for R , and we can write

$$C_R(\Gamma) = V_R T_R \left(H_R - \sum_{R' < R} C_{R'} H_R \right) \times J_{R1} \cdots \times J_{RN_R}. \quad (6.6)$$

The argument now falls into the general pattern already explained in Sec. III C, and we simply need to explain what are the jet factors J_i and the hard factor \hat{H}_N in Eq. (3.5). Their definitions follow from the definition of $C_R(\Gamma)$. The jet factors J_i are (sums over) unapproximated jet subgraphs, while the hard factor is obtained by summing the hard-scattering factor in Eq. (6.6) over all the relevant graphs:

$$\hat{H}_N = \sum_{\text{graphs}} V T \left(H - \sum_{R' < \infty} C_{R'} H \right). \quad (6.7)$$

The sum is over all (cut) graphs H for the cross section which have N outgoing parton lines. The unsubscripted T denotes the Taylor operator applied to the whole graph, i.e., that the whole graph is treated as a hard graph, and similarly for the veto factor V . The sum over regions R' is over all non-singular regions of H . Thus \hat{H}_N is the properly Taylor-expanded and subtracted hard subgraph with N external parton lines.

So far, we have merely made definitions that generalize the structures seen in examples. The factorized form on the right-hand-side of Eq. (3.5) is a trivial consequence of the structure of the Taylor expansion operator that we have already defined. The non-trivial part of

the proof of the factorization theorem is to prove that the remainder term is indeed power suppressed. What we need to show is that, to leading power, each individual graph is indeed the sum over the defined contributions for each of its leading regions:

$$\Gamma = \sum_R C_R(\Gamma) + \text{non-leading power.} \quad (6.8)$$

That is, we must derive an appropriate estimate for the non-leading-power term. To employ the factorization theorem in calculations, certain relatively simple subsidiary results will also be needed:

1. Infra-red and collinear safety of the subtracted hard scattering factors \hat{H} .
2. Infra-red safety of the *integrated* jet factors.
3. Renormalization-group-like equations for the scale dependence of the hard-scattering factors and the jets factors.

See Thm. 25 and Secs. VID and VIE.

The actual proofs will be relatively short. What will take the bulk of the space will be a series of definitions that provide a precise language for describing the various leading regions, their relations and the accuracy of the approximations. The main elements are:

1. The structure of the subtractions for each region. This is an obvious generalization from the examples, and the structure is common to many related problems, for example the construction of renormalization counterterms.
2. A precise characterization of the regions to be discussed.
3. A quantification of the errors. This needs a method of quantifying how close a point is to the defining surfaces of the various regions involved, which leads us to make a definition of the concept of a distance to a singular surface.
4. The actual construction of the error estimates. This involves considerations of the relative sizes of the virtualities of different lines, which will be characterized by the distances to singular surfaces.

One tricky point is that we will want to prove a suitable error estimate for a given graph given that the subtractions inside hard subgraphs actually work. The subtractions work if corresponding error estimates are available for the hard subgraphs. The simplest and most obvious proofs are made with the external lines of a graph on-shell. But when these same graphs occur as subgraphs of bigger graphs, we will in fact need the estimates for graphs with off-shell external lines, and the notion of distance to a singular surface needs to be carefully defined to allow for this possibility.

There will also be two views of the leading momentum regions. One will be a geometrical and topological view, of the kind illustrated by Fig. 9, which is symbolic of a momentum space of quite large dimension. In this view the key ideas are the distances to singular surfaces and the relations between the singular surfaces defined by set theoretic inclusion and intersection. The second view relates these regions to Feynman graphs, the sizes of the hard and jet subgraphs for different regions, as symbolized in Fig. 3. The error estimates are given by relating virtualities of lines in Feynman graphs to the distances to singular surfaces.

B. General formula for single graph

The structures seen in the examples suggest the general result. To make the argument self-contained and precise, I will give the results and proofs as a sequence of definitions and theorems. The first few recapitulate results from the previous sections.

Theorem 1 *The non-ultra-violet contributions to the cross section $\sigma[W]$ arise from neighborhoods of the pinch singular surfaces (PSS) for the massless theory. Moreover the leading-power contributions in our model correspond to the regions symbolized in Fig. 3. The corresponding PSS have groups of jet lines consisting of exactly parallel massless momenta.*

Proof: This was proved by Libby and Sterman [10] in their fundamental work on the analysis of the leading regions. A more recent account of the power-counting is given in [11].

This result applies to both real and virtual corrections to the process. In the case of loop diagrams, it is only necessary to consider regions where the (multi-dimensional) contour of integration is trapped near on-shell configurations for the virtual lines; otherwise the contour can be deformed. This accounts for the requirement that the singular surfaces correspond to a pinch. The momenta for external on-shell lines are, of course, necessarily pinched.

Definition 2 *The regions R for a graph Γ are specified by the corresponding PSS, with the inclusion of the limit points of the surfaces. In addition I define one other region, the purely ultra-violet region, whose associated surface is the surface where all the external lines of the graph are massless. I define a singular region to be one that corresponds to a non-trivial PSS; the only non-singular region is the ultra-violet region.*

This definition was explained and motivated by means of an example in Sec. VC. Recall that it was convenient to code each region by a set of points that is not the region itself but a related surface of singularity in a massless theory. The above definition is simply the natural generalization of the example.

One odd-looking feature is the definition of the surface associated with the purely ultra-violet region. For the example of the 4-parton graph of Fig. 4, this was R_4 , and in Sec. V its associated surface was defined to be the whole of the space of final-state momenta. But now we will also want to be able to discuss this graph when it is the hard subgraph for a particular region of a bigger graph. We will be using a Taylor expansion operator that replaces the external momenta of the hard subgraph by massless momenta. Therefore it is more appropriate to consider the space of momenta to be the space of all momenta (on-shell or not), and then the surface associated with R_4 is most naturally the surface where all the external momenta of the graph are massless. This surface then has an obvious embedding into a bigger space of momenta when the graph is a subgraph of a bigger graph. The above definition simply generalizes this idea to all graphs.

The inclusion of the limit points is an important technicality that lets us define the ordering of regions simply as set-theoretic inclusion. Physically the inclusion of limit points corresponds to including smaller regions in the definition of the defining surfaces. Initially, I found this to be contrary to my intuition. For example, in the case of Fig. 4 one might suppose the region R_2 where p_3 and p_4 are parallel should exclude the region where in

addition p_1 and p_2 become parallel. The approximation to this region provided by applying T_{R_2} certainly loses accuracy in the smaller region since it is no longer valid to neglect masses in the hard subgraph. However, the mathematics runs much more smoothly if one defines the surface that codes a particular region to include the surfaces that code each of the smaller regions.

Definition 3 *An ordering of the regions is defined by set-theoretic inclusion: $R_1 < R_2$ means that the defining surface for R_1 is strictly smaller than the defining surface for R_2 .*

It is convenient to make explicit the concept of a leading region:

Definition 4 *A leading region is a region that gives a leading-power contribution to the cross section. A non-leading region is a neighborhood of a PSS that gives a non-leading-power contribution.*

Theorem 5 *Feynman-graph interpretation of ordering for leading regions: Let R_1 and R_2 be two leading regions for a graph Γ . Then $R_1 < R_2$ is equivalent to saying that the hard subgraph, H_1 , for R_1 is smaller than the hard subgraph, H_2 , for R_2 . Correspondingly, when momenta approach the smaller region R_1 , some internal lines of H_2 have propagators with small denominators*

Proof: This is an elementary consequence of the meaning of the collinear kinematics of the singular surfaces: If R_1 is smaller than R_2 , then more lines of the graph have low virtuality in region R_1 than in region R_2 . Thus fewer lines are far off-shell and the hard subgraph is smaller.

Definition 6 *The approximation associated with a region R is notated by $T_R\Gamma$. In the case of a leading region, the definition of $T_R\Gamma$ was given in Sec. IV at Eq. (4.4). Observe that $T_R\Gamma$ is defined to extract the first term in the Taylor expansion in the masses of the external lines of the hard subgraph for the region, and then to use massless phase space for these external lines. (So it is not a naive Taylor expansion.) For a non-leading region, we define $T_R\Gamma = 0$.*

Theorem 7 *Basic properties of $T_R\Gamma$: The approximation $T_R\Gamma$ for a leading region R has the form of a hard subgraph $H(\hat{l})$, with massless external lines, times a product of jet factors, as in Eq. (4.4) or (6.2). The approximation can be expressed in terms of the original phase-space measure, as in Eq. (4.11), with the aid of a Jacobian factor. The Jacobian, Eq. (4.13), is analytic in a neighborhood of the surface R .*

Proof: These are immediate consequences of the definition, and all the necessary discussion is in Secs. IV A to IV C.

Definition 8 *Let Γ be a general graph for the cross section. Then the contribution $C_R(\Gamma)$ associated with a region R is defined recursively by Eq. (6.3). This is the appropriate approximation applied to the original graph minus the contributions associated with smaller leading regions. (Observe that for a non-leading region $C_R(\Gamma) = 0$, so that only leading regions need be considered explicitly.)*

It is convenient to define a related quantity, which is the original graph minus the contributions associated with smaller regions:

Definition 9

$$\overline{C}_R(\Gamma) = \Gamma - \sum_{R' < R} C_{R'}(\Gamma). \quad (6.9)$$

A trivial consequence is that

$$C_R(\Gamma) = V_R T_R \overline{C}_R(\Gamma). \quad (6.10)$$

A related definition is:

Definition 10 *For a graph Γ , we let $\overline{\Gamma}$ be the graph with subtractions made for all of its leading singular regions:*

$$\overline{\Gamma} = \Gamma - \sum_{R < \infty} C_R \Gamma. \quad (6.11)$$

(Only leading regions contribute, since otherwise $C_R \Gamma = 0$.) The notation $R < \infty$ means that the purely ultra-violet region is not included in the sum, i.e., that only singular regions are included in the sum.

For example, the singular regions for the graph of Fig. 4 are R_1 , R_2 and R_3 . In both of these two definitions, the bar over a quantity means that all subtractions are made except for the outermost one.

The notation defined by Def. 10 gives simple expressions for quantities we interested in. For example, applied to the hard subgraph for a particular region, it lets us write the contribution associated with the region as

$$C_R \Gamma = \prod_i J_{R_i} V_R T \overline{H}_R, \quad (6.12)$$

where H_R is the hard subgraph for a leading region R , J_{R_i} are its jet subgraphs, and \overline{H}_R is obtained from H_R by using Eq. (6.11).

It is perhaps worth reminding ourselves that $T \overline{H}_R$ is obtained from \overline{H}_R by

1. Setting the external lines massless and on-shell, and setting all the internal masses to zero, and
2. Inserting a Jacobian factor corresponding to the transformation between the exact momenta and the approximated massless on-shell momenta.

I will show that the sum of the contributions for the different leading regions gives the leading power behavior of Γ , so it is useful to make the following definitions:

Definition 11 *The asymptotic part of Γ is*

$$\text{Asy } \Gamma = \sum_R C_R(\Gamma). \quad (6.13)$$

Here the sum over leading regions includes not only the regions corresponding to leading singularities of the massless graphs, but also the purely ultra-violet region, where all the external lines of Γ are at wide angles.

The remainder is defined by any of the equivalent formulae

$$\text{Rem } \Gamma = \Gamma - \text{Asy } \Gamma = \Gamma - \sum_R C_R(\Gamma) = (1 - VT)\bar{\Gamma}, \quad (6.14)$$

where the unsubscripted T in the last form denotes the Taylor operator applied to the whole graph, i.e., where the whole graph is treated as a hard graph, and similarly for the veto factor V .

The main work of the rest of this section is to prove that the asymptotic part of Γ is indeed a good approximation to Γ , i.e., that $\Gamma = \text{Asy } \Gamma \times [1 + O(m^2/Q^2)]$ plus power-suppressed terms from non-leading regions, or, equivalently, that the remainder is power-suppressed: $\text{Rem } \Gamma = \Gamma \times O(m^2/Q^2)$, again up to power-suppressed contributions from non-leading regions.

The reason for making an explicit definition of $\text{Rem } \Gamma$ is that it unifies the treatments of leading and non-leading regions: We will prove that in all regions $\text{Rem } \Gamma$ is power suppressed.

In the following theorems our aim will be to give estimates of the sizes of various quantities and of the errors in approximations, just as we did in specific examples. Estimates will be propagated through further manipulations. The actual integrands of Feynman graphs have an enormous range of sizes; for example near a collinear configuration some propagator denominators get small. This happens in such a way that an integral over the region gives merely a logarithmic enhancement in the cross section. To avoid having to explicitly state the sizes involved every time, it is convenient to use a notation $\|\gamma\|$ for a previously derived estimate of some graph or subtracted graph γ . An example of such an estimate is Eq. (5.19), where for further manipulations in a general context, it would be useful to write $\|A - A_1\| = \|A\| M_{12}^2/Q^2$. The estimate of A , the unsubtracted graph itself, could simply be defined as the absolute value of A : $\|A\| = |A|$. Note that these estimates are functions of all the relevant kinematic variables and that we will require the estimates to be positive definite. In a theory with spin, there could be “accidental” zeros in the numerator factors; such accidental zeros should be removed from the definition of $\|\gamma\|$.

In addition it is convenient to define $L(\Gamma)$ to be a value that is leading twist in all singular regions of Γ —it differs from $\|\Gamma\|$ by being multiplied by a suitable dimensionless enhancement factor for each non-leading singular region.

Error estimates such as these involve some notion of distance to a singular surface, and we must of course define what we mean by a distance. Since there is no metric on the space of momenta over which we integrate, the definition is not unique, but for the purposes of error estimation, the precise choice of definition will not matter. A suitable definition can be constructed by starting with a choice of coordinates:

Definition 12 For each singular surface R , we choose “parallel” and “normal” variables. This means that we change the integration variables to have the form $(k_{\parallel}, k_{\perp})$, where k_{\parallel} is used to parameterize the surface R , and k_{\perp} are normal variables. Thus the surface R is $k_{\perp} = 0$, while the region corresponding to R is just a neighborhood of $k_{\perp} = 0$.

There is considerable freedom in the choice of these variables. One natural set for k_{\parallel} consists of:

- The longitudinal momenta of the lines in the jet subgraphs, divided by Q .
- The total energy of each jet, divided by Q .

- The angles between the external lines of the hard subgraph.

These variables are arranged to be dimensionless and to have a range of values of order unity; this will aid the use of dimensional counting to compute the dependence on Q .

The remaining variables, k_\perp , parameterize the deviation of momenta from the exactly singular configuration for the region. Given that we will wish to vary the virtualities of the external lines of a graph, an appropriate definition for the internal variables of a jet subgraph is given by the following steps:

- As in Sec. IV, let the total jet momentum for the subgraph be l_j^μ and let the final-state momenta be $p_{j,i}^\mu$.
- Use light-front coordinates for the momenta in the jet, in the overall center-of-mass frame, with the z axis being chosen as the direction of the jet's total spatial momentum \mathbf{l}_j . The $+$ and $-$ momenta of the final-state lines are $p_{j,i}^\pm = (p_{j,i}^0 \pm p_{j,i}^z)/\sqrt{2}$, and there are also four components of transverse momentum for each $p_{j,i}^\mu$. The axes are different for each jet subgraph.
- The fractional $+$ momenta, e.g., $p_{j,i}^+/l_j^+$, can be chosen to be among the parallel variables for the singular surface R , as listed earlier, in place of the longitudinal momenta of the lines in the jet subgraph.
- The $-$ momenta and the transverse momenta form the normal variables. (This applies both to the final-state momenta of the jet and to any loops.)

These variables have convenient properties under boosts along the jet direction.

We will also need to consider non-leading regions. These differ from leading regions by the possibility of extra lines beyond the minimum of two joining a jet subgraph to the hard subgraph and by the possibility of a soft subgraph connecting to the jet and/or hard subgraphs — see [1, 10]. The above definitions apply equally to the hard and jet subgraphs of non-leading regions, and we need only supplement them by adding the soft momenta to the list of normal variables k_\perp .

To define the notion of distance, we make the following definition:

Definition 13 *We write the normal variables k_\perp in terms of a single radial variable λ and some “angular” variables \tilde{k}_\perp . This can be done by writing $k_T = \lambda \tilde{k}_T$ and $k^- = \lambda^2 \tilde{k}^-/Q$ for each internal jet momentum, and $k^\mu = \lambda \tilde{k}^\mu$ for each soft momentum. Then we impose a suitable normalization condition on the scaled variables, for example, $\sum_{\text{jet } i} (\tilde{k}_{i,T}^2 + |\tilde{k}_i^- k_i^+ / Q|) + \sum_{\text{soft } i,\mu} |\tilde{k}_{\text{soft } i}^\mu|^2 = 1$. Thus the normal variables k_\perp have been expressed in terms of λ , and all but one of the scaled momentum components⁹. The scaling, for reasons explained below, is different between the transverse and $-$ components of jet momenta, and λ is arranged to have the dimensions of mass.*

⁹ Observe the difference between a subscript T and a subscript \perp . In this paper, the notation T will be used for the transverse components of ordinary Lorentz vectors, as usual, whereas the notation \perp will only be used to indicate the very different concept of a normal variable associated with a region of the space of all the momenta of a graph.

Since there is no natural metric on a space of several momentum variables, this choice of variable is not unique. But the details do not matter. It is the scaling properties with respect to λ and Q that will dominate our discussion. The normalization condition on the \tilde{k}_\perp variables is not Lorentz invariant; this is satisfactory since the power-counting method and the derivation of the singular regions rely on the use of a preferred rest frame.

The different scaling of the $-$ and transverse components of jet momenta is chosen so that the square of a jet momentum $k^2 = 2k^+k^- - k_T^2$ simply scales homogeneously, proportional to λ^2 . This will be convenient in constructing error estimates that rely on the virtualities of the lines of a graph. Observe further that the scaled variables are dimensionless with a range of order unity, and that λ ranges up to Q .

For an example of the meaning of the variable λ , consider the graph of Fig. 4. There are 14 variables of integration, which we split into 12 angular variables and the masses, M_{12} and M_{34} , of two pairs of particles. The graph is independent of the 12 angles, so we only need to consider the two pair masses.

In region R_1 we can define $\lambda_1 = \sqrt{M_{12}^2 + M_{34}^2}$. Since we have agreed to ignore the angles, there are no parallel variables for this region, and the normal variables consist of M_{12} and M_{34} .

In region R_2 , we can define $\lambda_2 = M_{34}$, and this is the only normal variable. There is one parallel variable, M_{12}/Q .

For the general case we can write the integral over a graph γ as

$$\int dk \gamma = Q^2 \int dk_\parallel \int d\tilde{k}_\perp \int \frac{d\lambda}{\lambda} \tilde{\gamma}(\lambda/m, \lambda/Q, k_\parallel, \tilde{k}_\perp). \quad (6.15)$$

Here we have taken advantage of the fact that the variables k_\parallel and k_\perp are dimensionless. The overall factor Q^2 corresponds to the dimension of the integrated graph. The remaining part of the Jacobian for the transformation of variables has been absorbed into the integrand to give $\tilde{\gamma}$, which is dimensionless. The mass-shell delta functions for the final-state particles are treated as part of the integrand. The integrals over k , k_\parallel and \tilde{k}_\perp are all multidimensional, of course.

The power-counting results of [10] tell us how $\tilde{\gamma}$ behaves as $Q \rightarrow \infty$ with λ , k_\parallel , and \tilde{k}_\perp fixed. The leading power occurs for the regions specified by Fig. 3, for which $\tilde{\gamma}$ goes to a generally non-zero constant:

$$\text{Leading region: } \tilde{\gamma}(\lambda/m, \lambda/Q, k_\parallel, \tilde{k}_\perp) \rightarrow \tilde{\gamma}(\lambda/m, 0, k_\parallel, \tilde{k}_\perp) \neq 0. \quad (6.16)$$

All other regions give a negative power of Q :

$$\text{Non-leading region: } \tilde{\gamma}(\lambda/m, \lambda/Q, k_\parallel, \tilde{k}_\perp) \sim \left(\frac{\lambda}{Q}\right)^p, \quad (6.17)$$

where the power p is, for the case of our model, at least 2.

Now λ ranges from 0 to order Q . When mass-shell constraints are allowed for, the minimum value is restricted to be of order m . When we perform the integral over all λ in a leading region, a logarithm results from the region $m \ll \lambda \ll Q$, whose coefficient is obtained by neglecting the mass in $\tilde{\gamma}$:

$$\text{Logarithm} = \int_m^Q \frac{d\lambda}{\lambda} \tilde{\gamma}(\infty, 0, k_\parallel, \tilde{k}_\perp). \quad (6.18)$$

Further logarithms result from the integrals over k_{\parallel} and \tilde{k}_{\perp} .

For a non-leading region, the integral over λ is roughly

$$\int_m^Q \frac{d\lambda}{\lambda} \left(\frac{\lambda}{Q} \right)^p, \quad (6.19)$$

which is dominated by $\lambda \sim Q$: the contribution from $\lambda \sim m$ is of order $(m/Q)^p$.

The primary operation in computing the asymptotics of a graph is the application of the Taylor expansion operator T_R for each region R . The definitions we have just made characterize this operator essentially as the extraction of the leading term in an expansion in inverse powers of Q , for large Q . The errors in the use of this expansion are associated with the neglect of λ and m with respect to virtualities in the hard subgraph for the region R . For a generic value of k_{\parallel} , the virtualities in H_R are of order Q^2 , and the errors have relative size λ^2/Q^2 . But when k_{\parallel} approaches values associated with smaller singular surfaces, some of the virtualities get smaller, and the errors get larger. To quantify this, it is convenient to define the distance of a point of momentum space from the defining surface of a region:

Definition 14 *Given a choice of normal and parallel variables for each R and of the overall scaling of the normal variables, we define the distance of a point k of momentum space to the region R as the value of $\lambda = \lambda(k, R)$.*

To estimate the errors in our expansion, etc., we need to relate the distance to a singular surface to the virtualities of lines of a graph.

Theorem 15 *Let k be a point of the momentum space for a graph Γ . Then the smallest virtuality, $V_{\min}(k)$, of the internal lines of Γ is at least of order the minimum of $\lambda^2(k, R)$ taken over all singular regions R of Γ . This means that the ratio $\min_{R < \infty} \lambda^2(k, R)/V_{\min}(k)$ is bounded: it is less than a constant that is independent of k .*

Proof: If we restricted our attention to *leading* singular regions, the proof would be quite simple, since in our theory, the leading regions correspond to groupings of external lines into jets. Then the distances to regions can simply be related, in order of magnitude, to the invariant masses of groups of external lines.

But complications arise since we will actually need to handle momenta in non-leading regions, and for them the scalings vary for different momentum components, and the relation to invariant masses is not so clear.

First, consider any particular singular region R . For generic values of k , the virtualities of the hard subgraph are of order Q^2 and the virtualities of the jet lines are of order $\lambda^2(k, R)$, if the region is a leading region, and hence without a soft subgraph. For non-leading regions there may be soft lines so that some jet lines get a virtuality of order $Q\lambda$. Hence for generic momenta at a distance λ from the region, the virtualities of internal lines of the graph are at least λ^2 .

However, by varying k_{\parallel} and k_{\perp} we can generally get lower virtualities, than the generic estimate, at a given value of λ .

Now fix k and find the singular region R_m that minimizes λ . It may be that k is a generic value for this region, in which case $V_{\min}(k) \gtrsim \lambda^2(k, R_m)$ and the theorem is proved. We will need to prove that no other possibility arises.

So suppose the opposite, that $V_{\min}(k) \ll \lambda^2(k, R_m)$. Then some lines of the graph have much lower virtualities than is given by the generic estimate. Let us call these ‘‘anomalous lines’’. Then we can make a *small* adjustment of k to put the anomalous lines exactly on-shell. But this corresponds to another singular region, R_n , say. Since some of the jet or soft lines of the original region R_m are in the hard subgraph of the new region, the new region is either larger or non-trivially overlaps with the previous one.

Because the anomalous lines of R_m , i.e., those with especially low virtuality, consist of all the jet and soft lines of the new region, we will be able to show that the distance to the new region R_n is less than the distance to the previous regions, R_m , contrary to the definition of R_m . Indeed, if k is counted as a generic momentum configuration for the new region R_n , then $V_{\min}(k) \gtrsim \lambda^2(k, R_n)$, which is just this result. If k is not generic, then we just repeat the above argument with R_m replaced by R_n .

Theorem 16 Accuracy of approximation given by T_R for a leading region. *Let γ be a graph, and let $\|\gamma\|$ represent an estimate of its size. Suppose k is a point which is a distance λ from the defining surface of one of its leading regions R , and suppose that the minimum virtuality of the lines in the hard subgraph H_R is $V_{H,\min}$. Then*

$$\gamma - T_R\gamma = \begin{cases} O\left(\|T_R\gamma\| \frac{\max(\lambda^2, m^2)}{V_{H,\min}}\right) & \text{if } \max(\lambda^2, m^2) \lesssim V_{H,\min}, \\ O(\|T_R\gamma\|) & \text{otherwise.} \end{cases} \quad (6.20)$$

The minimum virtuality $V_{H,\min}$ can be replaced by the square of the distance to the nearest singular surface smaller than R , if such a surface exists. Let us call this distance $M_B(k, R)$. If no smaller singular surface exists, or if the hard graph is a lowest-order tree graph so that it has no internal lines, then M_B is to be replaced by Q , and $V_{H,\min}$ by Q^2 .

Proof: The whole point of the definition of T_R was to make a useful approximation to a graph valid as $\lambda \rightarrow 0$, and this theorem formalizes how accurate this approximation is.

Now $T_R\gamma$ is obtained by replacing the hard subgraph for the region R by the first term in its expansion about the collinear limit for its external lines. The jet subgraphs are completely unapproximated, so that they do not enter into the error estimate. The errors come from three sources: (a) the neglect of the external virtualities for the hard subgraph in comparison with the virtualities of its internal lines, (b) the neglect of internal masses in the hard subgraph, and (c) in the calculation of the massless phase space measure, the neglect of the external virtualities of the hard subgraph in comparison with Q^2 .

The largest relative error comes from the internal lines of the hard subgraph that have the smallest virtualities; and these small internal virtualities arise precisely from neighborhoods of smaller regions than R . The error arises from neglecting both λ^2 and m^2 , so that we must insert the largest of these, i.e., $\max(\lambda^2, m^2)$ in the numerator of Eq. (6.20). Since terms neglected in the propagator denominators have factors of external virtualities and mass-squared, and since the virtualities of the external lines are proportional to λ^2 , the error term is quadratic, not linear, in λ and m .

When the minimum virtuality of the lines of the hard subgraph decreases below λ^2 or m^2 , the approximation to γ given by $T_R\gamma$ becomes totally inaccurate, and the error is simply estimated as 100% of the bigger of γ and $T_R\gamma$, which is normally the more singular quantity $T_R\gamma$.

Thus we have proved Eq. (6.20).

For the subsequent discussion, it is convenient to work in terms of the geometry of the momentum integration space and hence in terms of distances to singular surfaces. Small virtuality lines in the hard subgraph are obtained by letting the parallel variables k_{\parallel} for the region R approach the defining surfaces for smaller singular surfaces. The surfaces are smaller, because the regions of momentum are more restricted: the external lines are already of low virtuality, and we are finding places where additional lines have low virtuality. Then essentially the same argument that led to Thm. 15 shows that the minimum virtuality can be replaced by the square of the distance to the nearest smaller singular surface. This quantity repeatedly appears later, so we give it a name $M_B^2(k, R)$.

Of course, if there are no smaller singular surfaces, and, in particular, if the hard subgraph is a lowest-order tree graph, so that it has no internal lines, then the approximations involve the neglect of λ^2 and m^2 with respect to Q^2 . In this case we simply define M_B^2 to be Q^2 .

Theorem 17 Accuracy of approximation given by T_R times veto factor. *For any point k ,*

$$\gamma - V_R T_R \gamma = O\left(\|\gamma\| \frac{\max(\lambda^2, m^2)}{\max(M_B^2, \lambda^2, m^2)}\right). \quad (6.21)$$

Proof: This is the same theorem as Thm. 16, except that $T_R\gamma$ has been multiplied by the veto function defined earlier, and that in the error estimate $T_R\gamma$ has been replaced by γ .

The veto factor multiplying $T_R\gamma$ ensures that whenever we get close to the massless collinear singularities of $T_R\gamma$, this quantity is replaced by zero. In that case $\gamma - V_R T_R \gamma$ is just equal to γ , and a correct error estimate is just 100% of γ , instead of the commonly larger $T_R\gamma$.

The complicated looking denominator in Eq. (6.21) is just to combine the two cases in Eq. (6.20).

Definition 18 *In Thm. 16, the quantity M_B played an important role. So it is useful to formalize it and to make some related definitions. We consider a graph Γ and a point k of its momentum space. Then*

- $M_B(k, R)$ is the minimum distance to the defining surface of regions R' that are smaller than R : $M_B(k, R) = \min_{R' < R} \lambda(k, R')$. If there is no smaller region, then M_B is defined to be Q .
- $M_B(k, \Gamma)$ (with the argument being the graph Γ instead of a region R) is the minimum distance to a singular region of Γ . Thus, $M_B(k, \Gamma) \equiv \min_{R < \infty} \lambda(k, R)$.

- $M_{\text{ext}}(k, \Gamma)$ is the maximum of the square roots of the virtualities of the external lines of Γ .

The basic result that gives the error on our approximations is Thm. 16. Its simplest application is to a graph γ that has no singular regions. Then the only region is the ultra-violet region, and the difference between γ and $T_R\gamma$ only comes from the neglect of external virtualities with respect to Q^2 in the calculation of the phase-space Jacobian. This is equivalent to the observation that the value of λ^2 in Eq. (6.20) is of order the maximum external virtuality, i.e., M_{ext}^2 . If the graph has on-shell external lines, then the error is of relative order m^2/Q^2 , and therefore $\text{Rem } \Gamma = O(\|\Gamma\|m^2/Q^2)$.

To prove this result for graphs with non-trivial leading singular regions, we will use an inductive (or recursive) approach, proving the desired result on the assumption that suitable results for the errors of smaller graphs have been derived. The necessary results are conveniently stated with the aid of the following definition:

Definition 19 *A graph Γ is well-behaved if*

$$\bar{\Gamma} = O\left(L(\Gamma)\frac{M_B^2(k, \Gamma)}{Q^2}\right) \quad (6.22)$$

for all momenta k whenever the external momenta of Γ , which (for this definition) are not necessarily on shell, obey $M_{\text{ext}}(k, \Gamma) < M_B(k, \Gamma)$. Here, as defined by Eq. (6.11), $\bar{\Gamma}$ is the graph after subtractions for leading singular regions have been made. Also, as defined earlier, $L(\Gamma)$ is a quantity like $\|\Gamma\|$ modified so that it gives a leading contribution near every singular region.

More informally, we are defining Γ to be well-behaved if the subtracted graph $\bar{\Gamma}$ is power suppressed near every singular surface.

An equivalent formulation can be made in terms of the distances to individual singular regions. Thus Γ is well-behaved if

$$\bar{\Gamma} = O\left(L(\Gamma)\frac{\lambda^2(k, R)}{Q^2}\right) \quad (6.23)$$

for all regions R and for all momenta k whenever the external momenta obey $M_{\text{ext}}(k, \Gamma) < M_B(k, \Gamma)$.

The idea of this definition is that Γ may have singular regions, where it is substantially enhanced, and that without subtractions the integrals near the leading singular regions have strong logarithmic enhancements, which diverge if $m \rightarrow 0$. The aim of the subtractions that are used to define $\bar{\Gamma}$ —see Eq. (6.11)—is to provide a suppression in each of these regions. The above definition gives a criterion as to whether our definitions of the subtractions have succeeded in their aim, and so we will need to prove that all graphs are in fact well-behaved, in the sense of this definition—see Thms. 21 and 22. The ultimate results, including the factorization theorem will follow quite easily—see Thms. 20, 23 and 24, and Secs. VIA and VIC, etc.

For our proofs to work, we have to consider non-leading regions as well as leading regions, and the above definition also applies to them. By definition, to say a region is non-leading means that there is a power suppression near the defining surface of the region. There is no need of subtractions for non-leading regions, of course.

The restriction to $M_{\text{ext}}(k, \Gamma) < M_B(k, \Gamma)$ is needed, because once the external momenta get further off-shell than is allowed by this restriction, it becomes unnecessary to ask how close the internal momenta k are to the singular surface; the external virtuality has already forced some of the internal lines to have at least comparable virtuality.

The next theorem says that if all the leading singular regions of Γ have been properly subtracted, then a good approximation to the subtracted graph is obtained by applying a Taylor expansion to the dependence on its external momenta:

Theorem 20 *If Γ is well behaved and $M_{\text{ext}}(k, \Gamma) < M_B(k, \Gamma)$, then*

$$(1 - V_\Gamma T)\bar{\Gamma} = O\left(L(\Gamma)\frac{M_{\text{ext}}^2(k, \Gamma)}{Q^2}\right) \quad (6.24)$$

The left-hand-side is one of the equivalent forms of the definition of $\text{Rem } \Gamma$ —see Eq. (6.14)—so this theorem is just stating that the remainder is power-suppressed (or, as is often said, it is of higher twist).

Proof: T replaces the external momenta of $\bar{\Gamma}$ by on-shell massless momenta and replaces the internal masses m by zero. In addition it inserts a Jacobian factor for the transformation between massive and massless momenta. We now apply Thm. 17 to Γ when the region R is the purely ultra-violet region for Γ , to obtain:

$$\text{Rem } \Gamma = (1 - V_\Gamma T)\bar{\Gamma} = O\left(\|\bar{\Gamma}\|\frac{M_{\text{ext}}^2(k, \Gamma)}{M_B^2(k, \Gamma)}\right) \quad (6.25)$$

Here, we have used the fact that the distance to the defining surface of the ultra-violet region is of order M_{ext} . The desired Eq. (6.24) then follows from the meaning, Eq. (6.22), we gave to Γ being well-behaved.

More intuitively, this proof can be summarized as

- Away from all singular regions, the definition of T implies that a graph minus its Taylor expansion is suppressed by a factor of order M_{ext}^2/Q^2 , which is already the desired result, Eq. (6.24).
- As each singular region is approached, this suppression is worsened by a factor $Q^2/\lambda^2(k, R)$.
- But because the hard subgraph of each region is well-behaved, by the hypothesis of the theorem, $\bar{\Gamma}$ is itself suppressed by a factor $\lambda^2(k, R)/Q^2$ relative to Γ .
- The last two factors cancel each other.

Consideration of the worse case scenario for each value of k requires us to replace λ^2 by $M_B^2(k, \Gamma)$.

Although this proof looks quite trivial, there is actually one point that is particularly non-trivial. This is in the application of Thm. 17. That theorem applies most obviously to a graph or a function that is a simple product of propagators. But when the graph is a difference of relatively large quantities, the derivation requires more care.

A simple mathematical example for these results is provided by setting

$$\Gamma = \frac{1}{(m^2 + M_{12}^2)(m^2 + 2M_{12}^2 + Q^2)}, \quad (6.26)$$

where M_{12} is as an analog to a jet mass. The subtraction of the singular region $M_{12} \ll Q$ is accomplished by writing

$$\begin{aligned}\bar{\Gamma} &= \Gamma - T_1\Gamma \\ &= \frac{1}{(m^2 + M_{12}^2)(m^2 + 2M_{12}^2 + Q^2)} - \frac{1}{(m^2 + M_{12}^2)Q^2}.\end{aligned}\quad (6.27)$$

Here T_1 sets m and M_{12} to zero in the $1/(m^2 + 2M_{12}^2 + Q^2)$ factor.

The analog to Eq. (6.24) uses an operation T applied to $\bar{\Gamma}$, and in this model it consists of setting m to zero:

$$T\bar{\Gamma} = \frac{1}{M_{12}^2(2M_{12}^2 + Q^2)} - \frac{1}{M_{12}^2Q^2}.\quad (6.28)$$

There are relative errors of order m^2/M_{12}^2 in both terms separately. At first sight we only have

$$(1 - T)\bar{\Gamma} = O\left(\frac{m^2}{M_{12}^2}\right) \times \Gamma - O\left(\frac{m^2}{M_{12}^2}\right) \times C_R\Gamma,\quad (6.29)$$

which gives $O(\Gamma m^2/M_{12}^2)$. Since M_{12} may be much smaller than Q , this error may be much larger than the desired error, where the denominator in the error is Q^2 . However, the biggest parts of the errors are in fact identical, and this gives the correct result $O(\Gamma m^2/Q^2)$.

The general approach to this issue is to combine all the terms in $\bar{\Gamma}$ so that they are over a common denominator. Then the approximation is applied to each factor in turn, and hence the error is the relative error produced by the $1 - T$ operation times the size of $\bar{\Gamma}$.

Theorem 21 *Suppose all graphs smaller than Γ are well-behaved, in the sense of Def. 19, so that Γ is itself well-behaved.*

Proof: The structure of the proof generalizes the treatment of the concrete examples in Sec. V, and the proof will be illustrated with the aid of these examples.

If Γ is small enough that it has no singular regions, then $M_B = Q$ and $\bar{\Gamma} = \Gamma$. Then the definition of well-behavedness is trivially satisfied.

If Γ does have singular region(s), let k be any point for Γ that satisfies $M_{\text{ext}}(k, \Gamma) < M_B(k, \Gamma)$, and let R be the *nearest* singular surface. We put the other singular surfaces R' into the following classes:

- (a) $R' < R$,
- (b) $R' > R$,
- (c) R' intersects R , but it is neither a subset nor a superset of R ,
- (d) R' does not intersect R at all: $R \cap R' = \emptyset$.

Then

$$\begin{aligned}\bar{\Gamma} &= \Gamma - \sum_{R' < R} C_{R'}\Gamma - C_R\Gamma - \sum_{R' \text{ in (b-d)}} C_{R'}\Gamma \\ &= (1 - V_R T_R)\bar{C}_R\Gamma - \sum_{R' \text{ in (b-d)}} C_{R'}\Gamma,\end{aligned}\tag{6.30}$$

where we used Eqs. (6.9) and (6.10). We need estimates for each of these terms. Note first that if R is a *non-leading* region, then the subtraction term $C_R\Gamma$ for this region is zero, and thus that T_R is zero for a non-leading region. The necessary estimates for the terms corresponding to each class of R' are obtained as follows:

(a) From Eq. (6.12),

$$(1 - V_R T_R)\bar{C}_R\Gamma = (\text{jets of } R)(1 - V_R T_R)\bar{H}_R,\tag{6.31}$$

where \bar{H}_R is the subtracted hard subgraph of region R . Since H_R is a smaller graph than Γ , it is well-behaved, by the hypothesis of the theorem. Moreover, because R is the closest singular surface to k , the propagators with lowest virtuality are in its jet (or soft) subgraphs, and so $\lambda(k, R) \lesssim M_{\text{ext}}(k, H) \lesssim M_B(k, H)$. Hence Thm. 20 gives

$$(1 - V_R T)\bar{H}_R = O\left(L(H_R)\frac{\lambda^2(k, R)}{Q^2}\right),\tag{6.32}$$

and so

$$\begin{aligned}(1 - V_R T_R)\bar{C}_R\Gamma &= O\left(L(\Gamma)\frac{\lambda^2(k, R)}{Q^2}\right) \\ &= O\left(L(\Gamma)\frac{M_B^2(k, \Gamma)}{Q^2}\right),\end{aligned}\tag{6.33}$$

where the last statement follows since R is the closest singular surface to k , and the definition of $M_B(k, \Gamma)$ is that it equals the distance to the closest singular surface.

An example of this result is given by setting $R = R_2$ for Fig. 4. In this case, Eq. (6.33) states that $\Gamma - \Gamma_1 - \Gamma_2 = O(\Gamma M_{34}^2/Q^2)$ —as we saw at Eq. (5.42).

(b) Consider a singular region $R' > R$. We only need consider a leading region for R' , since otherwise $C_{R'}\Gamma = 0$. The definition of $C_{R'}$ gives

$$\begin{aligned}C_{R'}\Gamma &= V_{R'} T_{R'} C_{R'}\Gamma \\ &= (\text{jets of } R') V_{R'} T_{R'} \bar{H}_{R'}.\end{aligned}\tag{6.34}$$

Since $R' > R$ the hard subgraph of R' is a **bigger** graph than the hard subgraph of R , and some of the lines of the virtuality that determines R as the closest singular surface to k must lie in this hard subgraph of R' .

Moreover R' is a non-trivial singular surface, so its hard subgraph is smaller than Γ , so it is well-behaved, by the theorem's hypothesis. Since $T_{R'}\bar{H}_{R'}$ has

its external lines on-shell, we can apply the definition of well-behavedness to give

$$\begin{aligned} T_{R'}\overline{H}_{R'} &= O\left(L(H_{R'})\frac{\lambda^2(k, R)}{Q^2}\right) \\ &= O\left(L(H_{R'})\frac{M_B^2(k, \Gamma)}{Q^2}\right), \end{aligned} \quad (6.35)$$

from which follows

$$C_{R'}\Gamma = O\left(L(\Gamma)\frac{M_B^2(k, R)}{Q^2}\right). \quad (6.36)$$

An example is given by setting $R = R_1$ and $R' = R_2$ for Fig. 4. Then Eq. (6.36) states that $\Gamma_2 = O[\Gamma(M_{12}^2 + M_{34}^2)/Q^2]$.

(c) Suppose R' non-trivially intersects R . Just as in the previous case, we have

$$C_{R'}\Gamma = (\text{jets of } R') V_{R'} T_{R'} \overline{H}_{R'}. \quad (6.37)$$

We are considering a singular surface that is closest to k . In this region a certain set of lines has low virtuality. Now in the factor $T_{R'}\overline{H}_{R'}$, a certain other set of lines is set on-shell, and effectively this factor is being calculated in a neighborhood of the intersection of the two regions, $R \cap R'$. This case reduces now to case (b).

For Fig. 4, an example is given by setting $R = R_3$ and $R' = R_2$, so that $R \cap R' = R_1$, and Eq. (6.37) becomes $\Gamma_2 = O(\Gamma M_{12}^2/Q^2)$ —see Eq. (5.48).

(d) The final possibility is that $R' \cap R = \emptyset$. The definition of R implies that k is close to R . Now, in $C_{R'}\Gamma$, the hard subgraph $\overline{H}_{R'}$ has its external lines on shell, so k being near to R implies also that in the hard subgraph the momentum configuration is close to $R' \cap R$. But there are no such points.

We have shown that all the terms on the right-hand-side of Eq. (6.30) are of order $L(\Gamma)M_B^2(k, \Gamma)/Q^2$, and the theorem follows.

Theorem 22 *All graphs Γ are well-behaved.*

Proof: This is a simple consequence of mathematical induction applied to the previous theorem 21. If there are graphs Γ that are not well-behaved, then there is a minimal such graph. Application of Thm. 21 shows that the graph is well-behaved, contrary to hypothesis.

Theorem 23 *The remainder is power-suppressed for an on-shell graph:*

$$\text{Rem } \Gamma = O\left(L(\Gamma)\frac{m^2}{Q^2}\right). \quad (6.38)$$

Proof: From the definitions, $\text{Rem } \Gamma = (1-T)\bar{\Gamma}$, and from the previous theorem, Γ is well-behaved. Hence by Thm. 20

$$\text{Rem } \Gamma = O\left(L(\Gamma)\frac{M_{\text{ext}}^2(k, \Gamma)}{Q^2}\right) = O\left(L(\Gamma)\frac{m^2}{Q^2}\right). \quad (6.39)$$

It immediately follows that

Theorem 24 *Asy Γ is a good estimate of Γ up to power-law corrections, i.e.,*

$$\begin{aligned} \Gamma &= \text{Asy } \Gamma + O\left(L(\Gamma)\frac{m^2}{Q^2}\right) \\ &= \sum_R C_R \Gamma + O\left(L(\Gamma)\frac{m^2}{Q^2}\right). \end{aligned} \quad (6.40)$$

Theorem 25 *On-shell subtracted hard subgraphs $T\bar{H}_R$ are IR safe. That is, in the integral over final-state momenta, no collinear singularities result when two or more of the external lines of a hard subgraph become collinear.*

Proof: This theorem is, of course, essential for effective perturbative calculations. Because the masses of internal and external lines are set to zero by the T operation, the logarithmic enhancements in the collinear regions for the unsubtracted graphs become actual logarithmic divergences after the integral over final states.

The IR safety follows from the theorem that any graph, e.g., H_R , is well-behaved: for then, in the neighborhood of any of the singularities, \bar{H}_R has a power-law suppression compared with the unsubtracted graph.

C. Factorization for the cross section

We now have all the elements for use in the skeleton of the factorization proof in Sec. III C: a definition of $C_R(\Gamma)$ and a proof that the remainder in Eq. (3.3) is indeed power suppressed. The factorization theorem Eq. (3.5) has therefore been proved.

In Eq. (4.18), we expressed the factorization formula in terms of the phase-space integral for massless partons. Now we will reorganize this formula into a form that is particularly convenient for calculation, and especially for calculations by a MC event generator. It will consist of a hard-scattering cross section for making N partons multiplied by the probabilities for each of the partons to hadronize to a particular state. The sum over the (conditional) hadronization probabilities is of course to be unity,

To this end, we first define an integrated jet factor

$$Z(\mu_F/\mu_R, m/\mu_R) = \int \frac{dM_j^2}{2\pi} \int dL(p_j; l_j) \Theta(l_j^2/\mu_F^2) J_j(p_j). \quad (6.41)$$

As before, J_i is the sum over graphs of the form of Fig. 13, and we integrate it over all possible final states with the cut-off function $\Theta(l_j^2/\mu_F^2) = \Theta(M_j^2/\mu_F^2)$ restricting the range of allowed jet masses. This integral is performed in the rest-frame of the final-state of the jet,

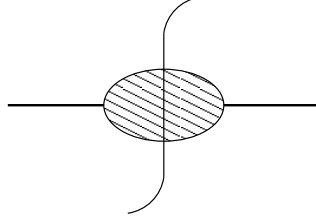


FIG. 13: Jet factor

i.e., we set $l_j^\mu = (M_j, \mathbf{0})$. The quantities μ_F and μ_R are the factorization and renormalization scales, and it is the cut-off function that gives the factorization scale its meaning, since nothing else in Eq. (6.41) depends on μ_F .

Next we define a differential jet factor as

$$dD(p_j; l_j; \mu_F) = dL(p_j; l_j, m) \Theta(M_j^2/\mu_F^2) \frac{J_j(p_j)}{Z(\mu_F/\mu_R)}. \quad (6.42)$$

This is the sum over fragmentation graphs completely differential in the phase space for the final-state particles. Note carefully that the phase-space measure dL contains the exact jet momentum l_j , not the approximated jet momentum \hat{l}_j . To allow a probability interpretation, a normalization factor $1/Z$ is present so that the integral of the factor over final states and masses is unity:

$$\int \frac{dM_j^2}{2\pi} \int dD(p_j; l_j) = 1. \quad (6.43)$$

(This integral is to be performed in the jet's rest frame.)

The hard scattering cross section is defined by

$$d\hat{\sigma}_N = K dL(\hat{l}; q, 0) \hat{H}_N Z(\mu_F)^N. \quad (6.44)$$

This is the sum of fully subtracted hard scattering graphs times a factor $Z(\mu_F)$ for each final-state parton. We have included the factor K , and a phase-space measure so that $d\hat{\sigma}$ really does have the normalization of a parton-level differential cross section. Observe that Z plays the role of a wave-function renormalization factor, just like the factor that would be obtained from the usual LSZ reduction method for a cross section. But note carefully that the correct procedure for calculating the hard-scattering cross section $\hat{\sigma}$ is to use the integrated jet factor $Z(\mu_F)$ in place of the residue of the propagator pole that would be indicated by the LSZ theorem.

With these definitions, the factorization formula Eq. (4.18) can be rewritten as

$$\sigma[W] = \sum_N \int d\hat{\sigma}_N(\hat{l}) \times \prod_{j=1}^N \int \frac{dM_j^2}{2\pi} \times \prod_{j=1}^N \int dD(p_j; l_j) \times W(f) + \text{non-leading power}. \quad (6.45)$$

In the last line we have a hard-scattering cross section $\hat{\sigma}_N$ and jet factors $dD(p_j)$. The integral over the jet momenta is expressed in terms of the massless momenta \hat{l} , since we will calculate the hard-scattering factor from massless on-shell graphs (with the aid of some subtractions); this results in the disappearance of the Jacobian Δ compared with Eq. (3.5).

The power-law correction in Eq. (6.45) is of order the cross section times m^2/Q^2 , with the usual addition of a term associated with non-leading regions.

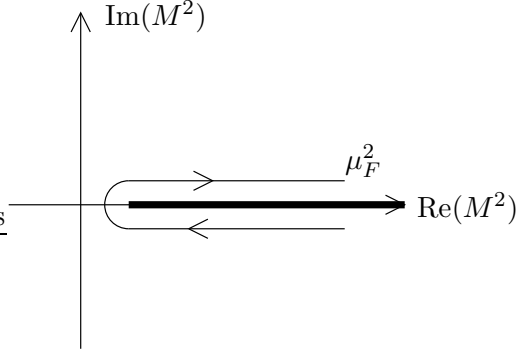


FIG. 14: Contour used to define the integrated jet factor $Z(\mu_F)$.

D. Infra-red finiteness of integrated jet factor $Z(\mu_F)$

The integrated jet factor $Z(\mu_F/\mu_R, m/\mu_R)$ defined by Eq. (6.41) is the integral of a cut propagator, Fig. 13. This implies that, even though the integrand includes small jet masses, the integral is infra-red safe for large μ_F , so that it is a good approximation to set particle masses to zero. The proof is the same as for an integral over the hadronic part of e^+e^- cross section and for other similar quantities [10]. It goes as follows: The integrated jet factor is the integral over the discontinuity of the uncut propagator divided by 2π :

$$Z(\mu_F) = \int_{C_1} \frac{dM^2}{2\pi} \Theta(M^2/\mu_F^2) S(M^2), \quad (6.46)$$

where the contour C_1 encloses the cut of the propagator $S(M^2)$, as in Fig. 14. The contour can be deformed into the complex plane to a region where the (complex) virtuality is of order μ_F^2 . Since the internal virtualities are now large, setting the particle mass m to zero is a good approximation that is valid up to a power-law correction.

In the above derivation, we have assumed that the cut-off function is a theta function $\Theta(M^2/\mu_F^2) = \theta(\mu_F - M)$. If a smoother function is used, minor modifications in the above demonstration are needed.

E. Renormalization group

Let us use the term “factorization scale” to denote the scale μ_F that appears in the cut-off function $\Theta(m^2/\mu_F^2)$ in the above formulae, and let the usual renormalization scale be μ_R .

The renormalization-group operator is, as usual,

$$\mu_R^2 \frac{d}{d\mu_R^2} = \mu_R^2 \frac{\partial}{\partial \mu_R^2} + \beta(g) \frac{\partial}{\partial g} - \gamma_m m^2 \frac{\partial}{\partial m^2}, \quad (6.47)$$

where γ_m is the anomalous dimension of the mass squared, and

$$\beta(g) = -\frac{3g^2}{512\pi^3} + O(g^5). \quad (6.48)$$

Then the integrated jet factor obeys

$$\mu_R^2 \frac{dZ(\mu_F/\mu_R; g(\mu_R))}{d\mu_R^2} = -\gamma(g) Z(\mu_F/\mu_R), \quad (6.49)$$

where the anomalous dimension of the parton field is

$$\gamma(g) = \frac{g^2}{768\pi^3} + O(g^4). \quad (6.50)$$

In QCD, the electromagnetic current is conserved and therefore has no anomalous dimension. It follows that the hard scattering factor, with the appropriate factors of $Z(\mu_F)$ is renormalization-group-invariant. However, in our model field the photon-parton coupling does not involve a conserved current and it in fact has an anomalous dimension. Thus the renormalization group equation for the strong-interaction part of the hard scattering coefficient does have an anomalous dimension:

$$\mu_R \frac{d(\hat{\sigma}_N/K)}{d\mu_R} = \mu_R \frac{d(\hat{H}_N)Z^N}{d\mu_R} = -\beta_e(g)\hat{H}_N Z^N = -\beta_e(g)\hat{\sigma}_N/K, \quad (6.51)$$

where β_e is an anomalous dimension associated with the electromagnetic coupling:

$$\beta_e(g) = -\frac{5g^2}{768\pi^3}. \quad (6.52)$$

VII. MONTE-CARLO ALGORITHM

A. Probabilities

To obtain a Monte-Carlo algorithm, we observe that when the weight factor $W(f)$ is omitted, the integrand of Eq. (6.45) gives the probability density of the final states. The weight factor W simply gave a convenient way of unifying the derivations of cross sections into a derivation of a total weighted cross section. Therefore we can obtain any cross section by the following technique: (a) omit the weighting factor $W(f)$, (b) multiply by the integrated luminosity, and (c) use a Monte-Carlo method to integrate and sum over the internal partonic variables (N , \hat{l} , and M_j) and over the hadronic final states. Recording the events generated by the Monte-Carlo integration, together with their weights allows us to construct any binned cross section.

Because of the factorization, the density for the final state is a product¹⁰ of

- A density for particular partonic final states (variables N and \hat{l}). This is given by the differential partonic cross section Eq. (6.44).

¹⁰ One annoying problem is that the cut-off on jet masses must be less than Q/N , for otherwise one can generate events that violate energy conservation. There are at least two solutions: (a) Set the cut-off μ_F to be smaller than Q/N_{\max} , where N_{\max} is the largest number of partons in the finite-order hard-scattering calculations that one actually uses. Then perform the somewhat complicated renormalization-group calculation that would enable the cut-off to be different for hard-scattering coefficients with different numbers of final-state partons. (b) Permit a higher cut-off, but veto events whenever they are generated with $\sum_j M_j > Q$. For consistency, a corresponding veto will need to be built into the subtraction terms in hard-scattering calculations. Note that the veto will only affect events in which a least one of the generated jets has an invariant mass of order Q .

- A (conditional) density for each jet mass M_j , given the partonic variables.
- A (conditional) density for the final-state for each jet, given its mass M_j .

Aside from the issue of negative weight terms, the densities are to be interpreted as probability densities, that is they sum and integrate to unity.

For determining the jet mass, it is convenient to define the integral over the jet factor J_i over its final states. With a normalization factor that will prove convenient, it is

$$F(M_j; \mu_R, m(\mu_R), g(\mu_R)) = \frac{M_j^2}{2\pi} \int dL(p_j; l_j) J_j(p_j; l_j; \mu_R, m(\mu_R), g(\mu_R)). \quad (7.1)$$

(The integral over the hadronic state is performed for a fixed value of the total jet momentum l_j^μ .) Apart from the normalization factor, this is just the cut propagator S , and it is simply related to the integrated jet factor:

$$F(M_j) = \frac{M_j^2 S(M_j^2)}{2\pi} = M_j^2 \left. \frac{\partial Z(\mu_F)}{\partial \mu_F^2} \right|_{\mu_F=M_j}. \quad (7.2)$$

Hence the massless limit can be taken for large jet masses: F is infra-red safe. Notice that F depends on the renormalization scale, but not on the factorization scale. Since it is proportional to a cut propagator, it has anomalous dimension γ :

$$\mu_R^2 \frac{dF}{d\mu_R^2} = -\gamma(g(\mu_R)) F. \quad (7.3)$$

Then the distribution of jet masses is given by

$$\frac{dP(M_j^2; \mu_F)}{dM_j^2} = \frac{1}{M_j^2} \frac{F(M_j^2; \mu_R) \Theta(M_j^2/\mu_F^2)}{Z(\mu_F/\mu_R)}. \quad (7.4)$$

This is renormalization-group invariant, since it is the quotient of two quantities with the same anomalous dimension.

If we set μ_F and μ_R to be of order Q , then a perturbative calculation of the hard scattering is valid. However the calculation of probability density for M_j suffers from large logarithms whenever $M_j \ll \mu_R$, so we must perform a renormalization group improvement for the calculation of the M_j^2 distribution. This enables F to be calculated with a renormalization scale M_j (a different scale for each jet):

$$\frac{dP(M_j^2; \mu_F)}{dM_j^2} = \frac{1}{M_j^2} \frac{F(M_j^2, M_j, g(M_j)) \Theta(M_j^2/\mu_F^2)}{Z(\mu_F/\mu_R)} \exp \left[- \int_{M_j^2}^{\mu_R^2} \frac{d\mu'^2}{\mu'^2} \gamma(\alpha_s(\mu')) \right]. \quad (7.5)$$

Observe that the renormalization scale μ_R has been replaced by M_j in the numerator F but not in the denominator Z . Then a finite-order calculation of F is valid provided only that $M_j \gg \Lambda$, so that $g(M_j)$ is small. Of course, if M_j is small, one must resort to phenomenological functions and models that are adjusted to fit data, just as in current event generators. I have set the renormalization scale to M_j for the jet, but any value of similar size would be equally good in principle. A somewhat smaller size would probably be best if the $\overline{\text{MS}}$ scheme is used, since the typical virtualities in the higher order calculation will be smaller than M_j^2 .

This formula is very similar to the formulae used in standard MC event generators. For example, the integral over the anomalous dimension corresponds exactly to the Sudakov form factor in the standard LLA formulation [2], with the anomalous dimension being an integral of the DGLAP evolution kernel over the splitting variable z . To leading order, the $1/Z$ factor can be replaced by its lowest order term, unity. Also, it can be verified that at leading (one-loop) order F is the anomalous dimension of the parton field:

$$F = \gamma(g) + O(g^4). \quad (7.6)$$

Thus the leading approximation to the distribution of M_j^2 is

$$\frac{dP(M_j^2; \mu_F)}{dM_j^2} = \frac{1}{M_j^2} \gamma(g(M_j)) \Theta(M_j^2/\mu_F^2) \exp \left[- \int_{M_j^2}^{\mu_F^2} \frac{d\mu'^2}{\mu'^2} \gamma(g(\mu')) \right] \left(1 + O(g(M_j)^2) \right). \quad (7.7)$$

However, if one goes beyond leading order some differences become apparent. The Z factor is no longer unity, and F is not the same as the anomalous dimension; both of these quantities are nevertheless perturbatively calculable (if μ_F and M_j are large).

So far we have discussed the hard scattering probabilities and the calculation of the values of M_j for each jet. The final ingredient is the distribution of the final states of a particular jet given M_j :

$$dJ = \frac{dL(p_j; l_j) J_j(p_j, M_j; \mu_R := M_j)}{F(M_j; \mu_R := M_j)}. \quad (7.8)$$

The denominator factor ensures that the integral over all final states is unity. In addition, the numerator and denominator have the same anomalous dimension, so that dJ is renormalization-group invariant. We may therefore set the renormalization scale to M_j , as indicated. Since the denominator is an integrated quantity with external mass M_j , it can now be calculated perturbatively without large logarithms. The numerator has an external mass M_j with an equal renormalization scale.

Because the numerator is exclusive, a fixed-order perturbative calculation suffers from large logarithms. However it is an object of the same type as the cross section that we originally tried to calculate: The problem of generating the final state from the fragmentation of the j th parton given its invariant mass M_j is essentially the same as the calculation of the final state of the whole event given Q . So we must recursively apply our algorithm to each jet.

To this end we need a factorization formula for the jet, and the only difference between this formula and the corresponding formula for the cross section is that the hard-scattering cross sections $d\hat{\sigma}_N$ are replaced by evolution kernels $d\hat{J}_N$:

$$dJ = \sum_N d\hat{J}_N \times \text{Jet factors}, \quad (7.9)$$

where the jet factor is the same as in Eq. (6.45). Note the sum rule:

$$\int \sum_N d\hat{J}_N = 1. \quad (7.10)$$

B. Algorithm

Since the number of variables to specify the final state is large, the use of Monte-Carlo techniques for the integration is appropriate. We have formulated the cross section as a product of factors, so that the following algorithm generates events with the correct probability distribution:

1. Generate a partonic final state according to the distributions given by the hard-scattering cross sections $d\hat{\sigma}_N$ defined in Eq. (6.44). Let the state contain N on-shell partons, and let their momenta be \hat{l}_j (for $j = 1, \dots, N$). If the hard-scattering cross sections are positive, then unweighted events can be generated, with the hard-scattering cross sections being treated as determining a probability distribution. If the hard-scattering cross sections are negative in some region, then appropriately weighted events must be generated.
2. For each parton j
 - (a) Choose a value M_j for the resulting jet, according to the distribution in Eq. (7.5).
 - (b) In the rest frame of the jet, construct the jet by a call to a showering algorithm. This starts at step 1, using the probability density $d\hat{J}_N$ in Eq. (7.9) instead of the probability density that corresponds to $d\hat{\sigma}_N$.
 - (c) In its rest frame, let the total momentum of the jet be $l_j^\mu = (M_j, \mathbf{0})$, and let the final-state hadron momenta be $p'_{j,i}$.
3. After all the jets have been constructed, apply a boost to each jet in the direction of its parent parton. Arrange the boost so that the total momentum of the jet in the overall center-of-mass frame obeys Eqs. (4.9) and (4.10).

In this algorithm, the showering of each parton is performed in the rest frame of the parton, with appropriate variables being the angles of the resulting partons. In contrast, many current event generators [2] use a momentum fraction variable, since the fragmentation is conceived of as being in a frame in which the partons are fast moving. The two views are necessarily equivalent.

In order to have a solution of Eq. (4.10) for λ , we must require that $\sum_j M_j \leq Q$. If we are to get results that are independent of the order in which the jets are fragmented, this implies that we must impose the condition $M_j \leq Q/N$ for each jet separately. This implies a maximum to the possible values of μ_F . Alternatively, as explained in footnote 10, we can apply a veto whenever $\sum_j M_j > Q$, and insert a corresponding correction in the subtraction terms in the hard-scattering coefficients.

As is usual in perturbative calculations we have a choice of renormalization scale, to which is now added a choice of the cut-off function $\Theta(M^2/\mu_F^2)$. The choice should ideally be made with the aim of minimizing the impact of higher-order uncalculated perturbative corrections. The cross-section is invariant under changes of this choice if the cross section and showering are calculated exactly.

But we have another choice in the algorithm. This is the correspondence between the approximated and unapproximated jet momenta at step 3. Any change in this correspondence amounts to a change of factorization scheme, and is compensated by corresponding changes in the subtraction terms that are used in the hard scattering cross section and in

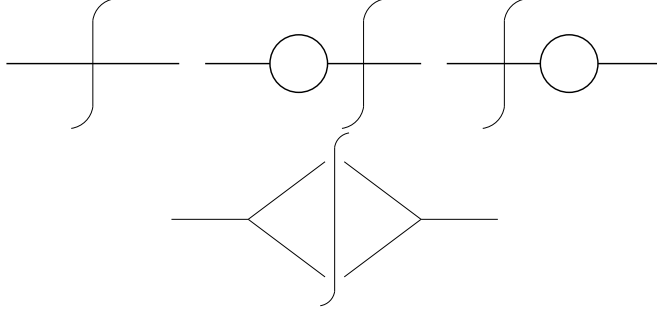


FIG. 15: Diagrams up to one-loop order for jet factor.

the splitting kernels. Such a choice always occurs in a Monte-Carlo event generator, but the necessity to construct a systematic algorithm for higher order corrections appears to me to restrict the range of simple choices.

The definition I have used—Eqs. (4.6)–(4.10)—seems to be the simplest if one requires that:

- Conservation of 4-momentum is obeyed at every stage.
- The renormalization of momenta is symmetric in the jets, and in particular it should not depend on the order in which the jets are fragmented.
- The fragmentation of a jet can be done independently of the momentum renormalization. This implies that the momentum renormalization amounts to a Lorentz transformation of each jet, but a different transformation for each jet.
- We must also allow for the possibility, in a more complicated theory than ϕ^3 , that there may be polarizations for the partons. In that case there are Lorentz spinors and vectors associated with the partons. To avoid complicating the Lorentz transformations that implement step 3 of the algorithm, we can require that the Lorentz transformations be simple boosts, for which the only natural direction is \mathbf{l}_j .

VIII. EXAMPLES OF CALCULATIONS

In this section I summarize the results of calculations that give the lowest-order quantities and the simpler next-to-lowest-order quantities. I assume throughout that the cut-off function defining the factorization scale provides a sharp cutoff:

$$\Theta(M^2/\mu_F^2) = \theta(\mu_F - M). \quad (8.1)$$

A. Integrated jet factor

Since the fully integrated jet factor is infra-red safe, it can be calculated in massless limit from the graphs of Fig. 15:

$$Z = \lim_{\epsilon \rightarrow 0} \int dM_j^2 \left\{ \left[1 + \frac{g^2}{768\pi^3\epsilon} \right] \delta(M_j^2) + \frac{g^2}{768\pi^3 M_j^2} \left(\frac{4e^{\gamma_E} \mu_R^2}{M_j^2} \right)^\epsilon \frac{\Gamma(5/2)}{\Gamma(5/2 - \epsilon)} \right\} + O(g^4)$$

$$= 1 + \frac{g^2}{768\pi^3} \left(\ln \frac{\mu_F^2}{\mu_R^2} - \frac{8}{3} \right) + O(g^4). \quad (8.2)$$

Here I used dimensional regularization with a space-time dimension $6 - 2\epsilon$. The last factor in the braces arises from the integral over the one-loop graph for real emission, and $\overline{\text{MS}}$ renormalization has been implemented by setting the bare coupling to be

$$g_0^2 = g_R^2 \left(\frac{\mu_R^2 e^{\gamma_E}}{4\pi} \right)^\epsilon (1 + \text{pure-pole counterterms}), \quad (8.3)$$

where the counterterms are poles at $\epsilon = 0$.

We also need the jet factor F for non-zero jet mass. In the massless limit in the physical space-time dimension, it is

$$F = \frac{g^2}{768\pi^3} + O(g^4). \quad (8.4)$$

As stated earlier, this equals the anomalous dimension γ at the leading order.

B. Distribution of partons in showering

The square of the order g graph for parton splitting gives a uniform angular distribution in the rest frame of the parent parton. Thus the lowest order for the splitting probability is

$$d\hat{J}_2 = \frac{d\Omega}{8\pi^2/3} + O(g^4), \quad (8.5)$$

where $d\Omega$ represents an element of solid angle in 5 space dimensions, and the denominator is the total 5-dimensional solid angle.

C. NLO hard-scattering coefficient

The two-parton hard-scattering cross section—see Eq. (6.44)—is obtained from the lowest-order graph of Fig. 1, from its one-loop virtual correction, and from multiplying the result by the square of the jet factor Z . The whole calculation is done in the massless limit and the result is

$$d\hat{\sigma}_2 = K dL(\hat{l}_1, \hat{l}_2; q, 0) \left[1 + \frac{g^2}{64\pi^3} \left(-\ln \frac{Q^2}{\mu_R^2} + \frac{1}{6} \ln \frac{\mu_F^2}{\mu_R^2} + \frac{14}{9} \right) + O(g^4) \right], \quad (8.6)$$

where K is the standard overall normalization factor for the cross section.

The lowest-order amplitude for the three-parton cross section is given by the sum of the three graphs in Fig. 16. Since we are computing the hard-scattering coefficient, the external momenta are the approximated, massless parton momenta, \hat{l}_i . Before subtractions, the squared amplitudes give

$$g^2 \left(\frac{1}{M_{12}^2} + \frac{1}{M_{23}^2} + \frac{1}{M_{13}^2} \right)^2. \quad (8.7)$$

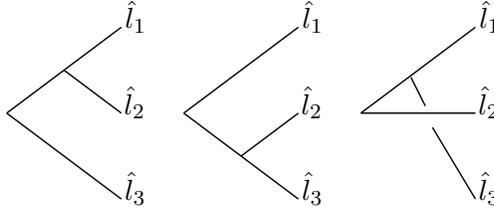


FIG. 16: Amplitude for three-parton production.

Here $M_{12}^2 = (\hat{l}_1 + \hat{l}_2)^2$, etc., are the masses of pairs of partons. When integrated over the parton kinematics, this squared amplitude would give the well-known logarithmic collinear divergences.

We have already calculated the subtractions for the square of one of the graphs in Sec. V B. There are two other terms, obtained by permuting the labels for the final-state partons. It is convenient to use the conventional dimensionless variables for the parton energies in the overall center-of-mass frame: $x_i = 2E_i/Q = 2\hat{l}_i^0/Q$. These lie in the range $0 \leq x_i \leq 1$, and they obey $x_1 + x_2 + x_3 = 2$. In terms of these variables the jet masses are $M_{12}^2 = Q^2(1 - x_3)$, etc. Then the final result for the subtracted, massless 3-parton cross section is

$$\begin{aligned}
 d\hat{\sigma}_3 = & K dL(\hat{l}_1, \hat{l}_2, \hat{l}_3; q, 0) \frac{g^2}{Q^4} \left[\left(\frac{1}{1-x_1} + \frac{1}{1-x_2} + \frac{1}{1-x_3} \right)^2 \right. \\
 & \left. - \frac{\Theta(Q^2(1-x_1)/\mu_F^2)}{x_1^3(1-x_1)^2} - \frac{\Theta(Q^2(1-x_2)/\mu_F^2)}{x_2^3(1-x_2)^2} - \frac{\Theta(Q^2(1-x_3)/\mu_F^2)}{x_3^3(1-x_3)^2} \right] \\
 & + O(g^4). \tag{8.8}
 \end{aligned}$$

The factors of x_i^3 in the denominators of the subtraction terms result from the Jacobians in the transformation between three-parton and massless two-parton kinematics, as explained in Sec. V.

IX. CONCLUSIONS

I have constructed a Monte-Carlo algorithm for e^+e^- annihilation in a model theory that can be applied at arbitrarily non-leading order (and hence includes arbitrarily non-leading logarithms). The main features are:

- Corrections to the hard-scattering cross section and to the kernel for parton showering are defined by a subtractive method to all orders of perturbation theory.
- The subtractions are applied point-by-point in momentum space, so that well-behaved functions are obtained that can be used in the calculation of arbitrary observables, without any restriction to infra-red-safe quantities.
- A modified LSZ prescription must be used for the normalization of the hard scattering coefficient (and the corresponding parton showering kernels). The normal LSZ prescription requires the on-shell amputated amplitudes to be multiplied by an appropriate power of the residue of the external parton propagator. Instead the on-shell amputated and subtracted amplitudes are to be multiplied by an appropriate power of an integrated jet factor.

- Exact momentum conservation is enforced at each stage, with a definite prescription for relating exact parton momenta to the corresponding approximated massless momenta that are used in the calculation of the hard-scattering and splitting coefficients.
- The produced jet masses are restricted by a cut-off function, and there is a renormalization-group-like invariance under changes of the cut-off function.
- The showering algorithm is rather different from a conventional showering algorithm. It is applied in the rest frame of the generated off-shell parton. The interpretation purely in terms of DGLAP kernels does not appear to hold beyond the leading-logarithm level.

Proofs were given that the errors are power suppressed. Thus the accuracy of the Monte-Carlo calculation is completely equivalent to that of conventional analytic calculations of inclusive processes, and so all the analytic (or matrix-element) results can be used, with a change of scheme, but now with the advantage of being able to treat arbitrary final-states. The method of proof appears to be capable of considerable generalization.

The use of a subtractive method to construct the corrections means that the subtracted higher-order corrections are not necessarily positive. So the algorithm must generally be used to generate weighted events. However, as explained in Ref. [5], adjustment of the cut-off function can be used to reduce the number of negative weighted events.

Of course, a model field theory is not QCD, and future work should aim at extending the results to QCD, as well as to lepto-production and hadro-production. The main problem here is well-known: that soft-gluon emission occurs at the leading power in any gauge theory, and the treatment of the leading regions needs to be considerable generalized. Unlike the case of inclusive cross sections, one cannot appeal directly to a cancellation of soft-gluon effects between real and virtual emission. One symptom of this problem is in the definition of the jet factor Z . In our model field theory it is given by a simple cut Green function of the parton field. But in a gauge theory, such a definition is not gauge invariant.

Collins and Hautmann [8, 9] have proposed some ideas at the one-loop level for how these subtractions should be performed in a way that allows gauge-invariant definitions of the jet factors and the similar initial-state parton densities. These definitions would represent a likely improvement on those by Collins and Soper [12].

Of course, coherent angular-ordered showering, such as is implemented in HERWIG, solves the problem of soft-gluon emission at the leading-logarithm level and somewhat beyond, but it does not represent a complete solution to the problem of obtain non-leading corrections in general.

Acknowledgments

This work was supported in part by the U.S. Department of Energy under grant number DE-FG02-90ER-40577. I would like to thank DESY and the University of Hamburg for their hospitality, and the Alexander von Humboldt foundation for an award during which this paper was completed. I would like to thank Gunnar Ingelman, Torbjörn Sjöstrand and

Dieter Zeppenfeld for useful conversations.

- [1] See the following, and references therein: R. Brock *et al.* [CTEQ Collaboration], *Rev. Mod. Phys.* **67**, 157 (1995);
 J.C. Collins, D.E. Soper and G. Sterman, “Factorization Of Hard Processes In QCD,” in “Perturbative QCD” (A.H. Mueller, ed.) (World Scientific, Singapore, 1989);
 R.K. Ellis, W.J. Stirling and B.R. Webber, “QCD and collider physics,” (Cambridge University Press, 1996).
- [2] G. Corcella *et al.*, *JHEP* **0101**, 010 (2001) [hep-ph/0011363];
 T. Sjöstrand, P. Edén, C. Friberg, L. Lönnblad, G. Miu, S. Mrenna and E. Norrbin, *Comput. Phys. Commun.* **135**, 238 (2001) [hep-ph/0010017].
- [3] M.H. Seymour, *Comput. Phys. Commun.* **90**, 95 (1995) [hep-ph/9410414];
 J. André and T. Sjöstrand, *Phys. Rev. D* **57**, 5767 (1998) [hep-ph/9708390], and references therein;
 G. Miu and T. Sjöstrand, *Phys. Lett. B* **449**, 313 (1999) [hep-ph/9812455];
 S. Mrenna, hep-ph/9902471;
 G. Corcella and M.H. Seymour, *Nucl. Phys. B* **565**, 227 (2000) [hep-ph/9908388].
 B. Potter, *Phys. Rev. D* **63**, 114017 (2001) [hep-ph/0007172].
 M. Dobbs and M. Lefebvre, *Phys. Rev. D* **63**, 053011 (2001) [hep-ph/0011206].
- [4] C. Friberg and T. Sjöstrand, hep-ph/9906316.
- [5] J. Collins, *JHEP* **0005**, 004 (2000) [hep-ph/0001040].
- [6] J.C. Collins, *Nucl. Phys. B* **304**, 794 (1988).
- [7] B.W. Harris and J.F. Owens, hep-ph/0102128;
 E. Mirkes and D. Zeppenfeld, *Phys. Lett. B* **380**, 205 (1996) [hep-ph/9511448];
 S. Catani and M.H. Seymour, *Nucl. Phys. B* **485**, 291 (1997), Erratum: **B510**, 503 (1997) [hep-ph/9605323];
 W.T. Giele and E.W. Glover, *Phys. Rev. D* **46**, 1980 (1992).
- [8] J.C. Collins and F. Hautmann, *Phys. Lett. B* **472**, 129 (2000) [hep-ph/9908467].
- [9] J.C. Collins and F. Hautmann, *JHEP* **0103**, 016 (2001) [hep-ph/0009286].
- [10] S.B. Libby and G. Sterman, *Phys. Rev.* **D18**, 4737 (1978);
 S.B. Libby and G. Sterman, *Phys. Rev.* **D18**, 3252 (1978).
- [11] J.C. Collins, L. Frankfurt and M. Strikman, *Phys. Rev. D* **56**, 2982 (1997) [hep-ph/9611433].
- [12] J.C. Collins and D.E. Soper, *Nucl. Phys.* **B194**, 445 (1982).